Fast 2D NMR for Metabolomics

Clément Praud, Marine P M Letertre, Arnab Dey, Jean-Nicolas Dumez, Patrick Giraudeau

13 Fast 2D NMR for metabolomics

Clément Praud[a], Marine P. M. Letertre[a], Arnab Dey[a], Jean-Nicolas Dumez[a], Patrick Giraudeau[a*].

[a]Nantes Université, CNRS, CEISAM UMR 6230, Nantes F-44000, France

*corresponding email address: patrick.giraudeau@univ-nantes.fr

ABSTRACT/WEB SUMMARY

Metabolomics provides crucial information on the metabolism of living organisms, by detecting and quantifying metabolites in biofluids, biopsies or extracts. Metabolomics studies involve analysing large collections of very complex samples by NMR or mass spectrometry methods. The resulting 1D spectra are characterized by the ubiquitous overlap between metabolite signals, justifying the need for the acquisition of 2D spectra on such samples. However, the long acquisition time of conventional 2D NMR makes it incompatible with the high-throughput nature of metabolomics, which explains why the acquisition of 2D spectra is generally limited to a subset of samples. In this chapter, we will describe how fast 2D NMR methods can lead to experimental times that become compatible with the systematic incorporation of 2D NMR in metabolomics workflows. Most frequently used 2D NMR methods include non-uniform sampling and ultrafast 2D NMR, but fast-pulsing methods and Hadamard spectroscopy have also shown some potential. In this chapter, we highlight how fast 2D NMR can facilitate the identification of biomarkers in untargeted metabolomics studies. We also discuss the use of fast quantitative 2D NMR strategies to provide accurate quantification of metabolites in targeted metabolomics approaches. Finally, we describe the promising combination of fast 2D NMR methods with hyperpolarization.

13.1. Introduction to Metabolomics

13.1.1. General background

Just like genomics aims to sequence and study the DNA contained in a complex mixture of organisms at a large scale, as transcriptomics does with RNA and proteomics with proteins, metabolomics aims to capture the broadest screenshot of the metabolites in complex biological samples.[1] Metabolites are defined as small molecules, which are end products and reactive compounds within cell regulatory reactions, usually weighting under 1,500 Da and pertaining to many different families. Those compounds can be endogenous such as short-chain fatty acids, steroids, lipids, organic or amino acids, sugars, *etc*, or exogenous, in which case they are found in the environment of the studied organism of interest, such as in the diet, a therapeutic treatment, the microbiome, or surrounding pollutants. These omics sciences are conceptually top-down approaches, which aim to holistically capture as much information as possible to understand how a biological system responds to a stimulus.[2] This is opposed to bottom-up approaches, for which analyses of a restricted part of the biological system of interest are performed to answer a specific biological hypothesis based on previous experimental data. Metabolomics is often considered as a particular omics science. First, it provides a link between genotypes and phenotypes[3] hence bringing invaluable information to understand dynamic biomolecular mechanisms occurring at different biological levels[4], and thus providing insights on the functionality of an organism, rather than just its capacity. Second, metabolomics is the most recent omics approach among the ones cited above. Still, metabolomics has already found numerous applications in personalized medicine[5–12] and epidemiology[13–15], pharmaceutical sciences[16–20], microbiome research[21,22], nutritional[23–26] and environmental sciences[27–33], exposome research[34–36] as well as in food quality control[37] for instance.

13.1.2. Untargeted Metabolomics, Targeted Metabolomics and Fluxomics

Through this entire chapter, the role of NMR in metabolomics, and especially the role of fast two-dimension (2D) NMR methods, will be discussed according to which metabolomics approach is applied. Indeed, metabolomics studies are usually classified into two main categories, depending on if the study is approached in an untargeted or a targeted fashion. A third category, for which fast 2D NMR techniques will push the boundaries of what is possible, and which seriously starts to gather attention, will also be considered through this chapter, the so-called stable-isotope resolved metabolomics (SIRM), also known as fluxomics. A general presentation and comparison of these three categories are provided below:

- Untargeted metabolomics requires no *a priori* on the detected metabolites. It aims at detecting spectral patterns from large datasets, which are analysed through statistical methods to highlight potential biomarkers. Detected metabolites depend on the limit of detection of the chosen analytical method, the physicochemical properties of the metabolites present in the sample and their degradation during sample collection, handling and preparation (see Figure 13.1).
- In targeted metabolomics, specific compounds of interest (*e.g.* one or several biomarkers, a class of chemically similar metabolites or a biological pathway) are quantitatively analysed (see Figure 13.1).
- Fluxomics allows the dynamic monitoring of intracellular biochemical reactions by quantitatively measuring fluxes in metabolomics pathways, following a stimulus and by focusing on the atoms of molecules which have been labelled thanks to the use of stable isotope precursors.

All three approaches are driven by biological questions and hypotheses. Untargeted metabolomics is by essence an exploratory top-down technique which is thus less biased than targeted assays as it covers a broader part of the metabolome (see Figure 13.1). However, data interpretation is often more complicated, especially the metabolite identification part

which is a major bottleneck in the metabolomics field. But once metabolite identification has been done and biomarkers have been highlighted, a targeted assay is often needed for biomarkers validation. As such, targeted metabolomics can be seen as a post-untargeted metabolomics strategy. Similarly, fluxomics can be seen as the final step following a targeted assay, during which concentration changes in metabolites are monitored in a continuous and dynamic way.

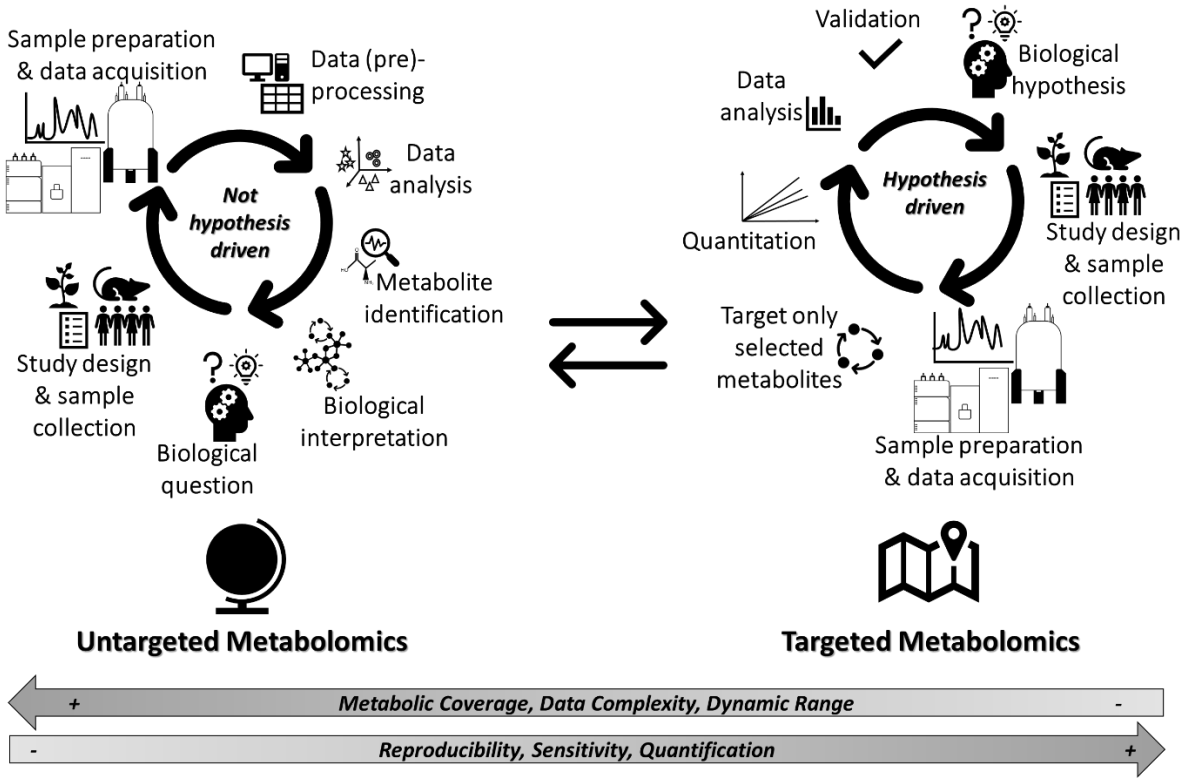

Figure 13.1 Untargeted and targeted workflows applied in metabolomics.

13.1.3. Metabolomics Workflow

Metabolomics is a very collaborative and interdisciplinary field which requires skills coming from different backgrounds to go through the consecutive steps. If we focus only on the untargeted approach in a first instance, the first step is to formulate a biological question, and to carefully define the most adequate study design, model organism and sample to collect, in order to answer the question in the broadest way possible, before preparing the sample and acquiring the data with the most adapted analytical strategy. As explained in the previous section, the aim of untargeted metabolomics being to capture as much information as possible, analyses generate extensively large datasets composed of many variables, which represent the metabolite signals present in each sample. These datasets are pre-processed and analysed with chemometrics techniques, based on either multivariate and/or univariate statistical analyses, to identify metabolites involved in a specific biological pattern (*e.g*. a signal presenting a high intensity in samples coming from a specific group). As explained above, once metabolites of interest have been highlighted, a targeted assay can be applied so that their absolute quantities get measured, followed by univariate statistics to validate or not the initial biological hypothesis that was experiment-driven (*e.g.* “Is the biomarker highlighted using this untargeted assay a real biomarker of this specific condition?”). Depending on the metabolites that need to be targeted, the choice of the analytical platform to use needs to be carefully considered.

13.1.4. Potential and limitations of NMR in Metabolomics

The two analytical foundations of metabolomics are NMR and mass spectrometry (MS), the latest often coupled to separative techniques such as liquid chromatography (LC), gas chromatography (GC), capillary electrophoresis (CE), or ion mobility (IM). Other spectroscopic techniques such as Raman[38] or Infrared[39] spectroscopy are also being applied in the field of metabolomics but for the sake of simplicity, NMR advantages and limitations will be discussed and compared only to MS-based metabolomics, as they have been the two main techniques driving the metabolomics forces for the past couple of decades. NMR was initially the most applied technique in the field of metabolomics, as it is simple and straightforward, especially in terms of sample preparation and metabolite identification. It also presents the advantage, compared to MS, to be a non-invasive technique and the sample, once analysed by NMR, can be recovered and analysed with another technique if needed. However, this advantage is counterbalanced by the two drawbacks of NMR spectroscopy: its lack of sensitivity and the signal overlap arising from sample complexity. Obviously, these drawbacks drastically limit compound identification and biomarker discovery. On the other side, MS is highly sensitive since only a tiny sample volume is requested for the analysis. Therefore, MS-based metabolomics became the most spread technique even if it is destructive.[40] Still, NMR has other core qualities to offer, which make this technique still very much applied in metabolomics. Among these qualities, we can cite its strong robustness, its high reproducibility, which give the possibility to study a large number of samples and to compare data acquired through time, on different spectrometers in different geographical locations.[41] This is much more difficult to reach for MS-based studies, especially without the rigorous use of quality controls.[42–44] Other advantages of NMR are the fact that 1D NMR, under carefully adjusted experimental conditions[45–47], is quantitative without the need to use calibration curves or labelled internal standards for each metabolites of interest, but with only one single external standard. NMR is also unbiased, provides structural information, and can be applied without extensive sample preparation and be easily interpreted. By considering those assets, NMR remains a particularly reliable analytical method, as highlighted, for instance, in applications to clinical metabolomics and personalized medicine.[10]

13.2. 2D NMR in Metabolomics

The overwhelming majority of NMR metabolomics experiments rely on one-dimensional (1D) proton-detected spectroscopy. 1D ^{1}H experiments are easy to implement and offer good sensitivity and throughput with a typical limit of detection in the micromolar range, in a few tens of minutes on high field instruments.[48] Therefore, 1D ^{1}H spectroscopy, associated with well-documented databases, is the tool of choice in most NMR metabolomics studies. Still, 1D ^{1}H NMR suffers from strong peak overlap issues, which are further compounded by a great diversity of metabolite concentrations. Such peak situations often prevent the unambiguous detection and identification of biomarkers in untargeted metabolomics, and also make it difficult to accurately quantify targeted metabolites. Several approaches are available to deal with this limitation. The decomposition of complex overlapped spectra into individual metabolite patterns is an efficient method.[49–51] However, it mostly relies on databases which are often specific to a given biological matrix (*e.g.* plasma, urine…) and sometimes require expensive commercial software. Alternatively, one can rely on ^{13}C NMR spectroscopy, whose extended chemical shift range considerably reduces peak overlap.[52] However, it results in a major sensitivity penalty -particularly at natural ^{13}C abundance- and often requires tailored NMR probes to improve the limit of detection. More recently, pure-shift ^{1}H NMR methods have emerged to collapse multiplets into singlets, hence reducing peak overlap.[53] Although some attempts have been made to apply pure-shift NMR in metabolomics, these methods suffer from low sensitivity and from the impact of strong coupling, which makes them quite impractical for complex diluted samples.[54,55]

Two-dimensional (2D) spectroscopy appears as a straightforward alternative for metabolomics.[56] First, it provides a better separation of overlapping peaks by spreading them along two orthogonal dimensions. Figure 13.2 illustrates such potential in the correlation spectroscopy (COSY) spectrum of a human urine sample. Second, it brings crucial structural information that can help identify unknown metabolites. Third, 2D NMR spectroscopy offers a diversity of homo- and hetero-nuclear pulse sequences that users can choose from to address their needs in terms of peak separation, resolution, sensitivity and throughput. Typically, homonuclear 2D experiments offer a good sensitivity but a sometimes-limited separation between overlapping peaks, while heteronuclear 2D experiments provide a better peak separation, albeit at the cost of a lower sensitivity due to the natural ^{13}C abundance.

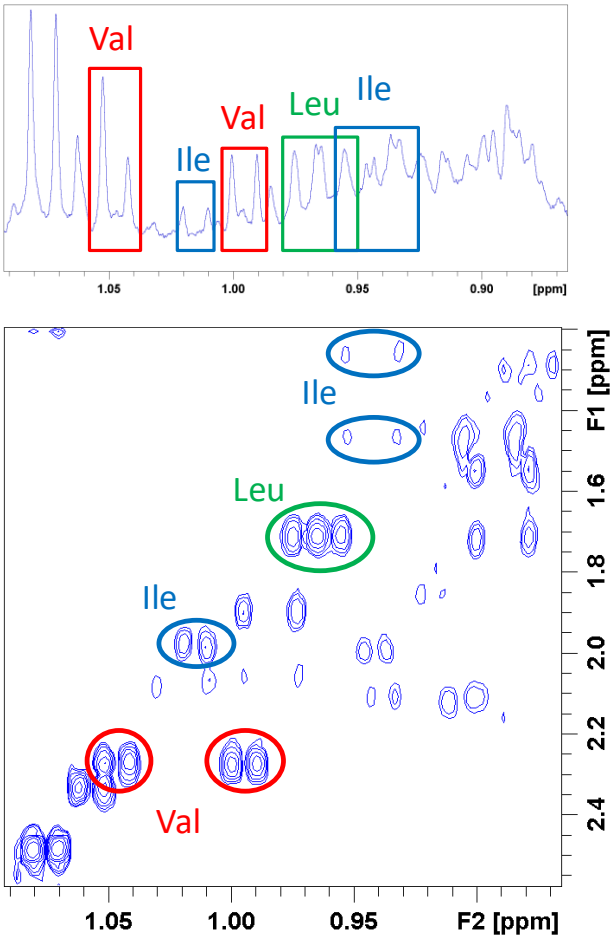

Figure 13.2 Illustration — in the case of urine — of the separation capabilities of 2D versus 1D NMR for metabolomics. Top: zoom of a ^{1}H 1D NMR spectrum obtained on a human urine sample at 298 K, with presaturation of the water signal through a 1D-NOESY (nuclear Overhauser effect spectroscopy) pulse sequence. The spectrum was acquired with 64 transients on a 700 MHz spectrometer equipped with a cryogenic probe. The signals from the identified metabolites are strongly overlapped, thus making their accurate quantification difficult. Bottom: corresponding zoom of a ^{1}H COSY spectrum for the same sample. The 2D spectrum was acquired with four transients and 300 increments in the indirect dimension, with the same hardware configuration. All the metabolites whose signals were overlapped on the 1D spectrum show at least one well-separated signal on the 2D spectrum, making their quantification possible. Val: Valine; Leu: Leucine; Ile: Isoleucine. Reproduced from Ref. [56] with permission Elsevier, Copyright 2017.

On the one hand, 2D NMR spectroscopy has been used since the early days of metabolomics to help identify metabolites after they had been highlighted as biomarkers through a conventional ^{1}H NMR metabolomics workflow.[57] In this case, 2D NMR spectra are recorded on a limited set of samples (and/or a fraction of the sample) for assignment purposes. Very advanced elucidation strategies have been developed along this line by Bruschweiler and co-workers, making use of cheminformatics, customized databases and even combined MS/NMR strategies.[58,59]

On the other hand, the systematic use of 2D NMR on larger series of samples is much more recent, mainly due to experiment time considerations that will be discussed in detail later in this chapter. Three main uses of conventional 2D NMR have been reported:

- The systematic use of 2D NMR in untargeted metabolomics, is associated with a classical bucketing of 2D peak volumes followed by statistical analysis. Van *et al.* were one of the first to show that 2D NMR (total correlation spectroscopy - TOCSY - with zero-quantum filtering - ZQF - in that case) could offer a better classification performance compared to 1D ^{1}H NMR, for the metabolic profiling of urine samples from mice.[60] Later on, Le Guennec *et al.* showed that 2D NMR could yield a similar group separation as 1D NMR in the case of model serum samples, but could provide much more accurate identification of relevant biomarkers.[61] Féraud *et al.* also demonstrated that 2D COSY spectra processed through multivariate approaches could provide a higher level of clustering than 1D NMR.[62] Other studies also showed that 2D NMR spectra acquired in metabolomics studies could also be processed with more advanced strategies, such as the hierarchical alignment of two-dimensional spectra-pattern recognition (HATS-PR)[63] or through image processing protocols to distinguish relevant signals through differential analysis by 2D NMR spectroscopy (DANS).[64]

- The use of 2D NMR for the targeted quantification of metabolites. Although 2D NMR peak volumes depend on a number of parameters (mainly J-couplings and relaxation times) owing to the multi-pulse nature of 2D experiments, several approaches have been developed to achieve absolute quantification from 2D NMR experiments. The first one is the calibration of the 2D peak response factors through external standards, which was demonstrated very early[65], and further illustrated in several targeted metabolomics studies.[66,67] The second one is the design of specific pulse sequences -variants of the heteronuclear single quantum coherence (HSQC) experiments- which provide 2D peak volumes that can directly be used for quantification relying on a single internal or external standard, as in quantitative 1D NMR.[21–23] The specificities of these quantitative 2D NMR approaches are described in Refs[56,68].

- The targeted determination of position-specific isotope enrichments in fluxomics. In this targeted approach, projections extracted from 2D TOCSY or HSQC spectra are used to access information on the repartition of isotopomers in complex biological samples such as extracts.[69,70] Such information is difficult to access from 1D spectra since the overlap between metabolite peaks is further complicated by multiple isotopic spectral patterns.

Despite the potential of 2D NMR for metabolomics and fluxomics, its use has been quite limited until 2010 or so, due to the long experiment time resulting from the need to sample the indirect dimension (t_1) with a sufficient number of increments to achieve a good resolution. Such long experiment times (typically several hours per spectra) were barely compatible with the high-throughput needs of metabolomics studies on large sample cohorts. Moreover, the long acquisition time of conventional 2D NMR was also shown to be detrimental to repeatability[71,72], owing to the impact of hardware instabilities in the indirect dimension that sometimes resulted in significant t_1 noise from most concentrated metabolites. Such limitations

have been largely circumvented by the development of fast 2D NMR methods, which have paved the way for many applications in targeted and untargeted metabolomics.

13.3 Where do we stand in the application of fast 2D NMR techniques within metabolomics and fluxomics?

Various fast 2D NMR approaches have been optimized and applied to metabolomics in the last decade, as described in Figure 13.3 where methods are divided into three main categories. The first one relies on pulse and delay manipulation strategies to reduce the repetition time between successive transients. The second one includes techniques that use different sampling strategies to reduce the number of increments in the indirect domain while trying to avoid penalties on resolution. Finally, the last family of strategies is based on spatial parallelisation of the second dimension in the so-called ultrafast (UF) method, allowing to record a 2D spectrum in a single-scan fashion.[73,74] Each category can be subdivided into different approaches as shown in the Figure 13.3**,** and as discussed in the following respective sections, starting with the pulses and delays manipulation strategies section.

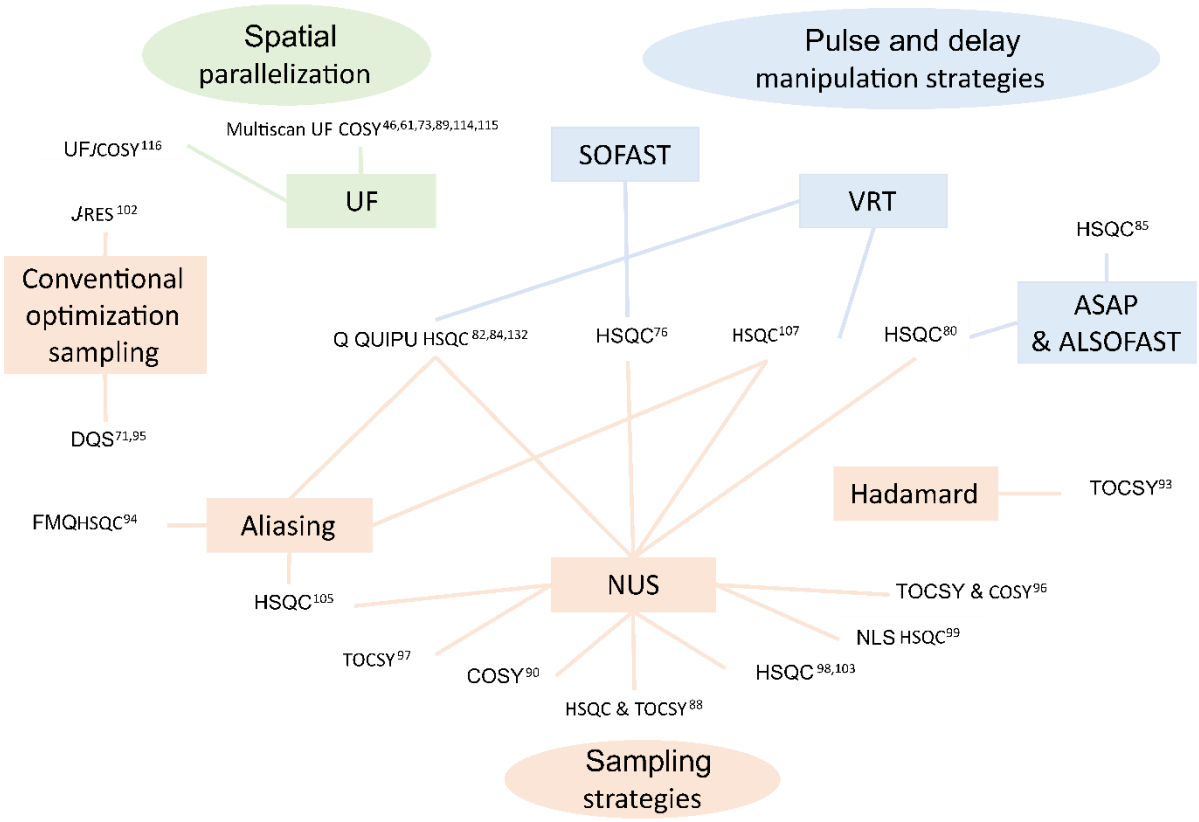

Figure 13.3 Main fast 2D NMR methods that were applied to metabolomics and fluxomics in the last decade, are discussed in the following sections. The three main families of techniques are represented, in blue for the pulse and delay manipulation strategies, in orange for sampling strategies and in green for spatial parallelization techniques. Rectangles correspond to the main methods that belong to each family. Coloured lines link specific publications to one or more time-saving strategies, as some applications, demonstrated in these publications, exploit several time-saving strategies in combination.

13. 3. 1. Pulse and delay manipulation strategies

13.3.1.1. Untargeted metabolomics

This section is dedicated to the application of untargeted metabolomics of fast 2D NMR methods that rely on the optimization of pulse angles and inter-pulse delays to reduce the

repetition time between successive transients. One of the first developed methods is called SOFAST for band-selective optimized flip-angle short transient. This selective approach relies on (i) using a reduced recycle delay, with an optimised excitation pulse angle (*e.g.*, using the Ernst angle) that enhance the available steady-state magnetization of the excited spins; (ii) accelerating the longitudinal relaxation of targeted protons of interest by leaving all other protons unperturbed. The latter cross-relax with the protons of interest via dipole-dipole interactions, thus considerably shortening the effective T_1 of relevant protons. Motta *et al.* proposed an encouraging proof of concept[75] in which SOFAST was used for real-time monitoring of ^{15}N-labelled living cells with SOFAST-HMQC (heteronuclear multiple quantum coherence) to obtain insight into metabolism behaviour of cells in specific conditions. Thanks to SOFAST, Ghosh and co-workers achieved a metabolomic study using SOFAST-HMQC combined with non-uniform sampling (NUS).[76] In their work, urine and plasma samples were investigated in an untargeted metabolomics workflow through which NUS and SOFAST strategies were used together to further reduce the experimental time without compromising the sensitivity of the resulting spectra. As a result, 20 peaks from plasma could be detected and 18 of them were assigned unambiguously, while 34 peaks could be detected for the urine samples from which 32 were assigned unambiguously. The resulting spectra highlight that the application of 35% NUS does not affect the peaks' resolution while reducing the experimental time. Combining NUS and SOFAST HMQC allowed to reduce the experimental time for serum and urine samples by 86% and 88% respectively in comparison with classical heteronuclear experiments. SOFAST HMQC spectra with NUS were recorded in 1 h and 15 min versus 9 h for conventional experiments. Very similar results were obtained for urine samples. Note that applications of SOFAST in metabolomics can generally benefit from a reduced recyle delay, but not from the enhanced longitudinal relaxation, which is restricted to specific situations, like for proteins where specific proton regions are targeted. In that case it is also a band selective approach that speeds up the relaxation of specific protons only.[77]

For small molecules where dipole-induced relaxation is much less efficient than in macromolecules, the ASAP (Acceleration by Sharing Adjacent Polarization) HSQC pulse sequence allows faster pulsing compared to SOFAST thanks to a spin-lock period placed during the recovery delay, which speeds up longitudinal relaxation via polarization transfer through scalar interactions.[78,79] Watermann *et al.* demonstrated an application of 2D ASAP HSQC in an untargeted metabolomics study. [80] The aim was to determine the geographical origin of 128 walnut samples based on 2D HSQC data supported by multivariate analysis, such as PCA (principal component analysis), various statistical models and confusion matrices, to discriminate different geographical groups (China, Germany and France). In this work, ASAP HSQC, combined with 25% NUS allowed to record a good quality 2D spectrum with 32 scans in 33 min. However, recording a classic HSQC (4h, 256 scans) prior to the study was necessary for comparison and assignments. Classification of different groups was similar with data from 1D and 2D NMR spectra. However, the loading plots appeared significantly improved using data coming from 2D experiments (see Figure 13.4) thanks to the additional signal dispersion brought by the ^{13}C dimension.

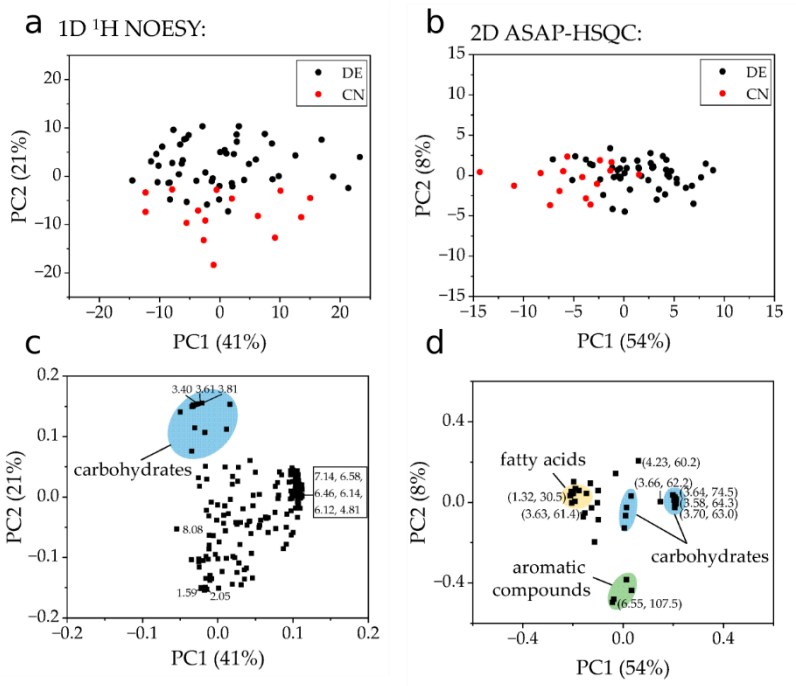

Figure 14.4 (a) PCA score plot of the differentiation of Chinese (CN) and German (DE) walnut samples using the 1D ^{1}H NOESY spectra with the corresponding loading plot below (c). Explained variance: PC1 = 41%, PC2 = 21%. (b) PCA score plot obtained by the ASAP HSQC spectra with the corresponding loading plot below (d). Explained variance: PC1 = 54%, PC2 = 8%. Adapted from Ref. [80].

13.3.1.2. Targeted metabolomics

As described in section 13.2, multiple attempts have been made in conventional 2D NMR to provide direct quantification of the metabolites of interest in targeted metabolomics. However, despite good analytical performance, conventional 2D NMR methods are not fast enough to deal with the high-throughput nature of metabolomics, especially when calibration procedures are required, which justifies the need for rapid acquisition methods. A few studies report the use of fast pulsing methods along this direction.

In 2018, Farjon *et al.*, optimized a quantitative 2D HSQC method providing direct quantification of metabolites of interest in a reduced experimental time.[81] This method was an upgraded version of a previously developed experiment called QUIPU (quantitative perfect and pure shifted) HSQC.[82] The original QUIPU experiment included several elements to yield absolute concentrations from HSQC spectra with a single internal reference, but was quite time-consuming. The accelerated version, Q-QUIPU (quick QUIPU) combines several time-saving strategies with quantitative pulse sequence elements like spectral aliasing, NUS and VRT (variable recycling time) to make it faster.[81] Principles of NUS and aliasing are discussed in more detail in section 13.3.2, but VRT is a strategy that belongs to fast-pulsing methods and is hence described here. With VRT, the 2D experiment starts with usual quantitative repetition times such as $T_r \geq 5T_1$, but is progressively reduced through successive t_1 increments and ends with $T_r \ll T_1$.[83] The list of decreasing repetition times follows a function (a decreasing exponential for instance) that is equal to unity for the t_1 increment where maximum signal is expected (the first increment for many 2D pulse sequences) to leave peak volumes unaffected. This built-in apodization reduces the experimental time of 2D NMR experiments by a factor of 5-10 while leaving peak volumes intact. Based on this accelerated quantitative method, metabolites in breast cancer cell extracts at mmol/L concentrations and below were quantified using lactate as an internal reference.[81] Each spectrum was recorded with an experimental

time of 5 h which corresponds to a significant time-saving compared to an experimental time around 32 h for the reference QUIPU spectrum.

More recently, Phuong and co-workers applied the Q-QUIPU HSQC methodology to quantify three major alkaloids in the root extract of goldenseal used as herbal supplements (see Figure 13.5).[84] They obtained an acceptable accuracy (<10%) in comparison with coupled UHPLC-MS/UV (ultra high-performance liquid chromatography) techniques and better sensitivity than standard HSQC. The authors demonstrated that the deconvolution of severely overlapped 1D peaks failed to provide accurate quantitative results, justifying the need for a quantitative 2D approach. Unfortunately, the reported experimental time was 2 days because a cryogenically cooled probe was not available at the time of the study. Otherwise, the expected acquisition time would have been comprised between 3 to 5 h.

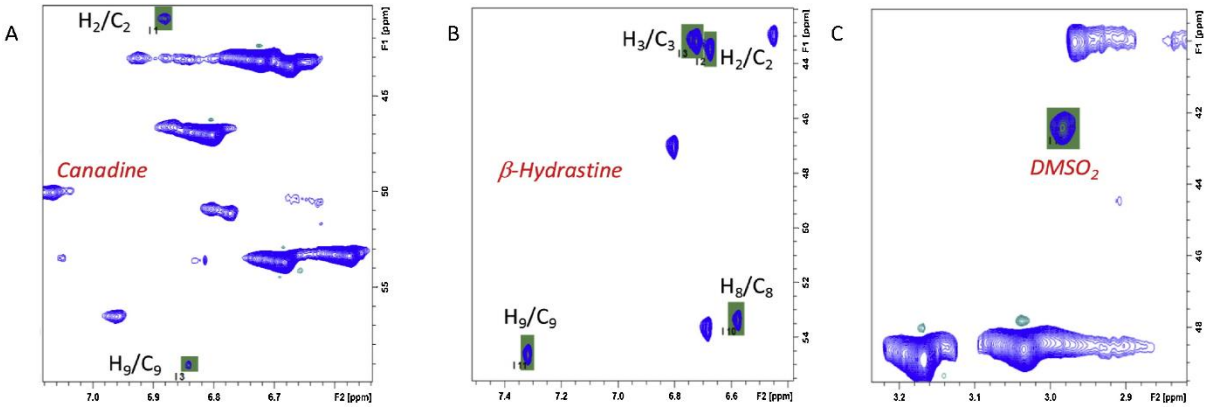

Figure 13.5 Application of the 2D Q QUIPU method to quantify alkaloids in root extracts. Parts of 2D Q QUIPU map showing canadine (A), *β*-hydrastine (B), and $DMSO_2$ (C) signals with the corresponding integration regions (green squares). $DMSO_2$ was used as an internal reference. Reproduced from Ref. [84] with permission from Elsevier, Copyright 2018.

13.3.1.3. Fluxomics

While fast-pulsing strategies have not much been applied to the field of fluxomics, an application of ALSOFAST was reported in 2018 by Schätzlein *et al.*[85] ALSOFAST is an alternative SOFAST sequence, in which the heteronuclear multiple quantum coherence of interest is excited with a classical INEPT (insensitive nuclei enhanced by polarization transfer) pulse cascade instead of the frequency-selective pulse used in SOFAST.[86] Schätzlein *et al.* applied an ALSOFAST-HSQC pulse sequence to investigate the effect of different kinds of antioxidant gold nanoparticles on a HeLa cancer cell model grown on a ^{13}C glucose-enriched medium, but also to monitor glucose metabolism in the cell model and study the antioxidant effect of the coated gold nanoparticles. Highly resolved ^{1}H-^{13}C-HSQC spectra using the ALSOFAST-HSQC pulse sequence were acquired, revealing the position-specific isotope patterns of the corresponding ^{13}C-nuclei from carbon multiplets with a reduced experimental time of 30 min for ^{13}C labelled cell extracts. Data were processed with chemometric multivariate tools such as OPLS-DA (orthogonal partial least squares discriminant analysis). HeLa cell extracts treated and untreated with nanoparticles were statistically discriminated and relevant metabolism pathways could be highlighted.

13.3.1.4 Discussion

Fast pulsing methods are just starting to be assessed for metabolomics applications. SOFAST and ALSOFAST make it possible to use short inter-scan delays, although they only benefit from enhanced longitudinal for systems in which spin diffusion is an effective relaxation mechanism, such as macromolecules or small molecules in viscous solvents.[75] ASAP allows to reduce even more the interscan delay, to a few tens of microseconds, although the short

recovery delay (associated with the use of spin-lock between each scan for ASAP) imposes a certain demand on the RF coil. In all cases, these techniques are restricted to heteronuclear experiments. On the other hand, VRT is more modest in terms of time reduction compared to the techniques cited above, but it can still provide significant time savings. However, the function defining the decrease of the repetition time through successive t_1 increments needs to be adapted to the system under study. The potential of these methods for metabolomics remains to be fully assessed, and is likely to be complementary to the sampling strategies described in the next section.

13. 3. 2. Sampling strategies

13.3.2.1. Untargeted metabolomics

Here, we highlight the application of alternative sampling strategies to untargeted metabolomics. Most examples concern the use of NUS, one of the most popular approaches to reduce the experimental time in 2D NMR. Instead of acquiring all the indirect data points as in conventional 2D experiments, only a randomly selected fraction of these points is sampled, and the spectrum is then obtained by relying on dedicated reconstruction algorithms.[87] The percentage of experimental points recorded is chosen by the operator before the experiment. As a consequence, a “25% NUS” experiment will have only 25% of the total number of points that are sampled, resulting in a quarterly reduction of the experiment time. NUS offers the opportunity, starting from any conventional experiment with typical acquisition parameters, to reduce the experimental time, or to improve the resolution in the indirect dimension without any penalty on the experiment time. Several studies have shown that NUS levels of about 20–30% per dimension can yield appreciable time savings in metabolomics without compromising on spectra quality.

In 2014, Le Guennec and co-workers investigated the potential of using NUS as a way to accelerate 2D NMR for untargeted metabolomics.[61] The study aimed to identify biomarkers of colorectal cancer to help diagnose and control such disease. Synthetic model samples containing 30 metabolites were used to mimic the composition of serum of patients affected by colorectal cancer. Half of them were prepared as control samples and the rest mimicked the serum of cancer patients. Various 2D NMR methods were used and compared in this work: NUS HSQC and NUS DQF (Double Quantum Filtered) COSY, and multi-scan UF COSY. The latter approach is discussed in more detail in section 13.3.3.1. Here, we focus on results obtained from NUS. NUS DQF COSY spectra were recorded with 30% NUS, leading to an experiment time of *ca.* 35 min versus the original experiment which lasted almost 2 hours. NUS HSQC spectra were recorded with 50% NUS leading to an experimental time of *ca.* 29 min versus 1 hour for the conventional version. Spectra were then bucketed and submitted to supervised statistical analysis (OPLS-DA). Since the composition of model samples was completely known, results could be compared to an OPLS-DA calculated from metabolite concentrations, used as a ground truth. Authors observed that NUS-accelerated 2D NMR provided the same group separation as conventional 2D NMR for the metabolomics study of biofluids, but in a shorter time. Most importantly, the authors demonstrated that the loading plots obtained from 2D NMR data were closer to the ground truth than those obtained from 1D NMR data, thanks to the reduced peak overlap, and that buckets from specific biomarkers were more uniquely identified from 2D datasets.

In a subsequent study, the same authors further investigated the performance of NUS to record very high-resolution HSQC and TOCSY spectra on a mixture of standards.[88] They showed that both HSQC and TOCSY spectra could be recorded with a very high resolution and no penalty in terms of sensitivity, highlighting the fact that NUS can either be used to

reduce the experiment time or to improve the resolution, providing a highly needed flexibility in the analysis of complex mixtures.

In 2018, Marchand and co-workers developed an untargeted lipidomic fingerprinting workflow applied to a chemical food safety issue.[89] Lipidomics is a part of metabolomics that focuses on the lipid fraction of the metabolome. The study aimed at detecting the forbidden use of a growth promoter in livestock. Ractopamine diet-fed pig samples were investigated versus control samples to highlight specific lipidomic patterns. The authors used two fast NMR approaches: ^{1}H NUS ZQF-TOCSY and ^{1}H UF COSY. NUS results are discussed here, whereas UF COSY results are discussed in section 13.3.3.1. 50% NUS was used to record the NUS ZQF-TOCSY spectra, leading to a total experimental time of 1 h 47 min. The NUS proportion was selected to ensure a sufficient number of signals recorded without reconstruction artefacts. The choice of the ZQF-TOCSY was driven by the clean in-phase resulting line shapes and the high number of observable correlations. Both correlation and diagonal peaks were integrated. PCA was then performed from 2D buckets as shown in Figure 13.6. 2D bucketing was facilitated and more reliable, compared to 1D bucketing, thanks to the better separation provided by the 2D spectrum. As in the previously mentioned study, the authors showed that the group separation obtained on the PCA score plot was similar with 2D NMR compared to 1D NMR, but they demonstrated that the loading plot obtained from 2D NMR data provided a less ambiguous identification of relevant biomarkers, compared to 1D NMR data.

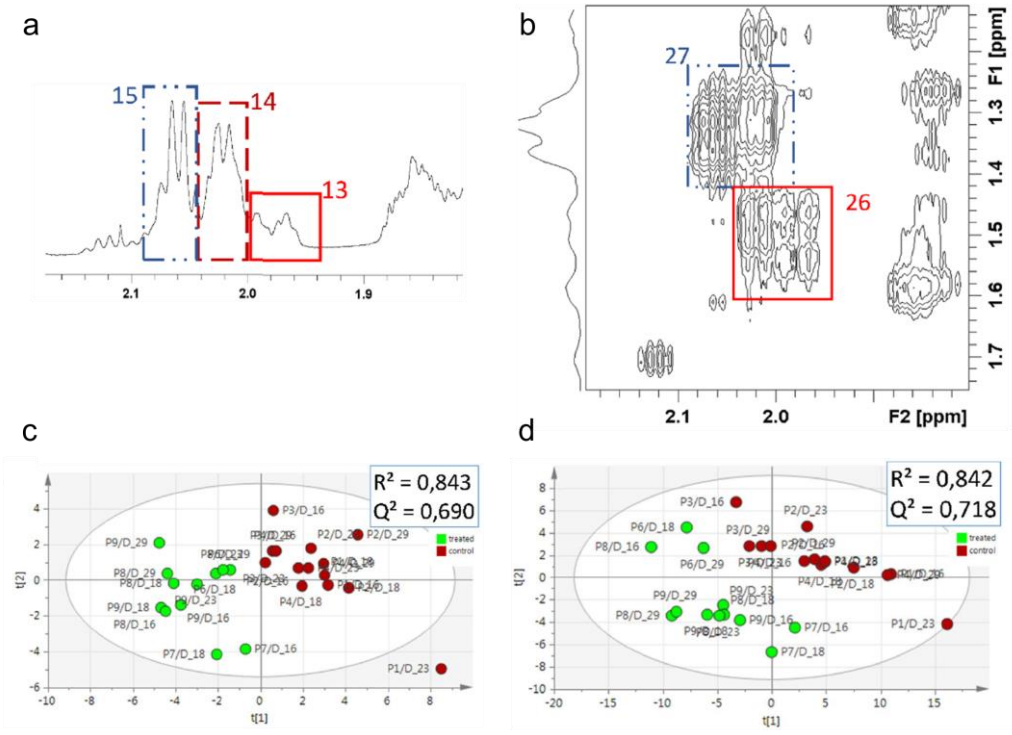

Figure 13.6 NMR lipidomics from pig serum lipid extracts, comparing ractopamine diet-fed pigs (green) with control pigs (red). (a, b) Zooms on specific bucketing regions in spectra from pig serum lipid extracts. (a) Bucketing from a 1D spectrum. The bucket n°15 contains the –CH2–CH=CH signal from fatty acyls (FA); the bucket n°14 contains both the –CH2–CH=CH signal from FA and CH (C12) from cholesterol and esterified cholesterols (Chol/CholE); the bucket n°13 contains the CH (C7) from Chol/CholE. (b) Bucketing from a ZQF-TOCSY spectrum. The bucket n°27 contains the –CH2–CH=CH signal from FA whereas the bucket n°26 contains the CH (C12) and CH (C7) from Chol/CholE. (c, d) PLS-DA score plot of the lipidomics study of ractopamine in pigs from: (c) 1D data and (d) 2D NUS ZQF-TOCSY data.

Associated R^2 and Q^2 values are specified within each box. Each dot represents an individual (*i.e.* a sample) and is labeled as PXX/D_YY corresponding to the pig number (P) and the sampling day (D). Green dots correspond to the Treated group whereas red dots correspond to the control group. Adapted from Ref. [89] with permission from Springer, Copyright 2018.

In 2020, Féraud et al., reported an untargeted metabolomics study on biofluids with the use of NUS applied to a ^{1}H COSY pulse sequence.[90] Samples from three different urine donors were taken on four successive days, with each time two dilution levels. Eight measures were performed for each donor sample which led to a total of 72 spectra collected with three experimental conditions: conventional COSY with either 4 or 1 scans, and COSY with 1 scan and 50% NUS. Corresponding experiment times were 50, 13 and 8 min, respectively. Several NUS levels were initially tested and 50% NUS appeared to provide the best time/sensitivity compromise. Data obtained were then statistically analysed through PCA combined with two different data analysis workflows.[91] Fast COSY provided very similar results compared to the initial COSY, but in a reduced time. Also, donor samples were differentiated thanks to PCA and accelerated 2D approaches showed efficient group discrimination, as good as conventional COSY but in a shorter time.

Hadamard spectroscopy exploits an alternative sampling strategy to reduce the experimental time of 2D NMR[92,93] It relies on polychromatic selective inversion or excitation pulses, to select multiple signals and impart them with a specific phase. Between sub spectra, the phase of the individual signals is changed to obtain Hadamard-encoded spectra which can be unambiguously reconstructed using a Hadamard transformation to obtain sub spectra for individual compounds. Hadamard TOCSY was used by Ludwig and co-workers, who reported consequent time savings: less than 20 min for Hadamard TOCSY versus 18 h for conventional TOCSY, without any loss of sensitivity.[93] They studied 38 colorectal cancer cells extract and 8 adenoma cells samples, to attest the potential of the method in metabolomics. The analytical performance of the method was investigated on 19 control samples. All results were submitted to unsupervised multivariate analysis (PCA) to highlight specific statistical groups. The results allowed to find relevant metabolic signatures that could discriminate one cancer type from another and to map the associated metabolomic pathways. However, Hadamard spectroscopy is not as straightforward as NUS to implement, since it requires setting selective pulses based on a priori knowledge of the spectral patterns. This probably explains why the application of Hadamard spectroscopy to metabolomics remains scarce in the literature.

13.3.2.2. Targeted metabolomics

For targeted metabolomics, several papers were published that relied on conventional 2D NMR approaches, but with a clever optimization of the indirect spectral width and number of increments to reduce the experiment time. In 2007, Lewis and co-workers published one of the very first papers reporting the potential of 2D NMR for targeted quantitative analysis.[66] Their fast metabolite quantification (FMQ) strategy combined ^{1}H-^{13}C NMR HSQC and aliasing to quantify targeted metabolites. Aliasing is an efficient method to reduce the number of points needed to sample the indirect dimension, by deliberately violating the Nyquist condition.[94] In the FMQ approach, quantitative HSQC spectra were collected in 128 increments using a 70 ppm spectral width in the indirect dimension (versus 140 ppm for a conventional HSQC). Aliasing was optimized to avoid overlap between 2D peaks. By using a calibration approach, the authors were able to quantify 40 metabolites in biological samples such as plant extracts from *Arabidopsis thaliana*, *Saccharomyces cerevisiae*, and *Medicago sativa.* The method showed 2.7% of accuracy on absolute concentrations in only 12 minutes per spectrum.

While spectra aliasing is well suited to relatively sparse heteronuclear 2D spectra, it is a less adapted solution to shorten the duration of homonuclear 2D experiments since aliasing would result in significant peak overlap. However, the duration of homonuclear 2D experiments can also be shortened by careful optimization of the number of increments in the indirect dimension, and some pulse sequences are particularly well adapted to such optimization. In

2011 Martineau *et al.* attempted to reduce as much as possible the number of t_1 increments in the case of 2D ^{1}H INADEQUATE (incredible natural abundance double quantum transfer experiment) or Double Quantum Spectroscopy (DQS) for targeted metabolomics.[71] DQS is particularly relevant for the analysis of complex metabolic mixtures since strong diagonal signals are removed, thus limiting both peak overlap and dynamic range issues. This also makes it possible to drastically reduce the number of indirect acquisition points, leading to significant time savings. Martineau *et al.* showed that DQS spectra could be obtained on breast cancer cell extracts in 7 min with 64 t_1 increments. A repeatability better than 2% was achieved for metabolite concentrations as small as 100 µM, together with a great linearity. Interestingly, the authors reported a significant improvement in repeatability when reducing the experiment time, as a result of a lower impact of hardware instabilities. Following these results, E. Martineau *et al.* showed the application of DQS to the absolute quantification of a series of breast cancer cell extracts thanks to a standard addition procedure.[95] 2D NMR quantification results on extracts made it possible to highlight quantitative biomarkers of breast cancer cell line types.

As for untargeted metabolomics relying on alternative sampling schemes, NUS is one of the most popular methods to accelerate targeted metabolomics workflows. In 2018, von Schlippenbach *et al.* performed a detailed optimization and evaluation of NUS parameters for the targeted analysis of urinary metabolites by homonuclear 2D NMR.[96] NUS ^{1}H-^{1}H-TOCSY and NUS ^{1}H-^{1}H-COSY with a 45° coherence transfer pulse were combined to standard addition experiments. Different NUS sampling schemes and reconstruction algorithms were evaluated, leading to acceptable repeatability (CV – coefficient of variation - around 10%). In 2020, Jiang *et al.* reported a similar strategy combining NUS with a TOCSY pulse sequence to analyse plant extracts.[97]

NUS has also been efficiently employed to shorten the duration of heteronuclear quantitative 2D NMR experiments. In 2020, Zhang *et al.* investigated the analytical performance of NUS HSQC combined with calibration for quantification purposes. They determined the concentration linearity and limits of detection and quantification (LOD and LOQ) of several common metabolites.[98] LOQ of these common metabolites were obtained in the low µmol/L range. Almost all investigated metabolites displayed a correlation coefficient better than 0.9 which indicated an excellent linearity. However, the repeatability was quite disappointing in some cases (with CV up to 35% on less concentrated samples). An alternative approach to obtain absolute quantification by combining HSQC with NUS was presented by Rai and Sinha in 2012.[99] Authors reported an almost 22-fold reduction time for the acquisition of 2D HSQC spectra in comparison with classic 2D NMR and without any compromise in the quantification capability of low concentration metabolites. Here, absolute quantification was achieved by calculating a correction factor for each 2D peak of interest, based on relaxation times and *J*-couplings, to retrieve the correct concentration of the corresponding metabolites, an approach previously described by the same group.[100] With this strategy, authors successfully quantified metabolites in native and lyophilized human urine samples.

13.3.2.3. Fluxomics

In fluxomics, one of the main strengths of NMR is to be able to measure multiple position-specific isotope enrichments in a single experiment.[101] A common approach relies on the integration of ^{13}C satellites in ^{1}H NMR, but it is significantly limited by peak overlap. One way to improve signal discrimination at a reasonable time cost is the 2D heteronuclear *J*-resolved (*J*-RES) pulse sequence. As explained by Cahoreau and co-workers, the spectral complexity is reduced thanks to *J*-RES by dispersing heteronuclear scalar couplings in the second dimension while preserving the ^{1}H NMR sensitivity.[102] Since only scalar couplings are sampled in the indirect dimension, it leads to significantly reduced experiment durations. Cahoreau *et al.* used heteronuclear *J*-RES to measure isotopic patterns from ^{13}C-enriched metabolite

mixtures and non-labelled model mixtures, and biomass extracts from bacterial cultures. Experiment times were comprised between 15 to 30 minutes.

In 2017, Lee *et al.* investigated the potential of NUS HSQC to perform carbon isotopomer analysis on cell extracts and living cells.[103] 25% NUS led to an approximate experimental time of 2 h, versus 8 h for conventional HSQC. Carbon multiplet patterns of aspartate were analysed to get insights into the metabolic usage of acetate by L210 cells, thanks to the high resolution provided with the NUS HSQC pulse sequence.

Accessing position-specific isotope information can also be relevant at natural isotopic abundance, a field where the high precision of NMR is absolutely crucial. Indeed, 0.1% repeatability is required to accurately sample the variations of natural isotopic abundance. While SNIF (Site-specific Natural Isotopic Fractionation)-NMR was used for decades to authenticate the origin of pure molecules[104], its application to complex samples is much more recent. In 2016, Merchak *et al.,* opened a new field called “metabisotopomics” in 2D NMR, at the border between metabolomics and isotopomics.[105] This one relies on studying both insights provided by metabolomics, such as relevant biomarkers, and by isotopomics, the latter being defined as the determination of multiple isotopic parameters at natural abundance. Exploited together, these data can bring complementary information on sample origins. However, 2D NMR methods are required to face the sample complexity, since peak overlap would considerably impact the precision. In 2013, Martineau *et al.* showed that ^{1}H-^{13}C HSQC spectra recorded with spectral aliasing and processed with linear prediction could yield a repeatability of 0.2%.[106] In 2016, Merchak *et al.* went a step further by simultaneously investigating the metabolomic and isotopic profiles of triacylglycerol matrices using a fast ^{1}H-^{13}C HSQC 2D NMR method.[105] Spectral aliasing was used in combination with NUS to decrease the long experimental time and improve the resolution, respectively. Investigations were done on 32 commercial vegetable oils to classify them according to their botanical and geographical origins. An excellent precision (a few per mil) was reached in only 22 min. A few years after, Haddad and co-workers applied a similar strategy to analyse small quantities of cholesterol at natural abundance in cheese.[107] A ^{1}H-^{13}C HSQC method combining NUS, linear prediction (LP) and VRT, was used to reduce the acquisition time, while the use of adiabatic pulses improved both sensitivity and precision. The method allowed to record a 2D HSQC map in 31 minutes with long-term repeatability of 2 per mil and relative standard deviation always below 0.5%.

13.3.2.4 Discussion

Contrary to the pulse and delays strategies described in the previous section, fast sampling strategies are more general, easy to implement and can be applied to most 2D pulse sequences. As described before, aliasing allows the reduction of the overall experimental time, but the time-saving is limited by the factor by which one can reduce the indirect spectral width to still have a decent and exploitable spectrum with no 2D peak overlaps. A careful optimization of the number of t_1 increments is also possible without aliasing, but the reduction of the experiment time is limited by the truncation of the free induction decay (FID), even if linear prediction can help. NUS is probably the most efficient alternative sampling method to reduce the number of t_1 increments in the indirect domain. However, the performance of NUS is limited by the efficiency of the reconstruction algorithms[87] which can lead to a loss of repeatability, which can be detrimental to metabolomics analyses. The above-mentioned examples particularly highlight this limitation in the case of heteronuclear experiments at natural ^{13}C abundance. Still, the combination of NUS and aliasing, when carefully implemented, can lead to appreciable time savings that can be crucial in high-throughput metabolomics and fluxomics.

13. 3. 3. Spatial parallelization (UF 2D NMR)

Spatial parallelisation consists of acquiring different sub-experiments simultaneously, from different slices of the sample.[108] Among spatial parallelisation methods, UF NMR is an efficient way to speed up the acquisition of multi-dimensional experiments.[108–110] Most popular UF 2D NMR pulse sequences rely on a continuous encoding scheme combining frequency-swept pulses with magnetic field gradient pulses, followed by an echo-planar spectroscopic imaging (EPSI) acquisition block derived from magnetic resonance imaging (MRI). This strategy allows to record a 2D map in a single-scan fashion and in less than 1 second. Considering the high throughput demand of metabolomics, spatial parallelisation appears to be a good candidate to overcome conventional and fast 2D NMR approaches acquisition time limits. Despite this, the application of UF 2D NMR to complex mixture analysis, and in particular to metabolomics and fluxomics, needs to account for specific limitations.[111] First, UF 2D experiments are overall less sensitive than their conventional 2D experiment counterparts. A typical limit of detection for single-scan UF COSY can be estimated at 1 mmol/L at 600 MHz, which only allows the detection of major metabolites. This lower sensitivity can be mainly imputed to the large bandwidth filter used to cover the high dispersion induced by magnetic-field gradient pulses during acquisition. Other parameters such as spectral widths and resolution are interdependent and also limited by hardware demands. Therefore, multi-scan variants of UF 2D NMR have been suggested and appear to be better suited to metabolomics. They consist in simple scan accumulations to improve the signal to noise ratio (SNR), and/or interleaving several EPSI acquisition trajectories to increase the available spectral width.[112] In metabolomics, such approaches have been mainly reported for the COSY pulse sequence, one of the most sensitive 2D experiments, as described below.

13.3.3.1. Untargeted metabolomics

In 2014, Le Guennec and co-workers evaluated for the first time, the potential of the multi-scan UF strategy for untargeted metabolomics[61] relying on the method described in the first place by Pathan *et al.*[113] As discussed in section 13.3.2.1, in which NUS results were presented, authors designed a set of model metabolite samples mimicking the composition of serum from patients affected by colorectal cancer, in order to provide a ground truth for the evaluation of fast 2D methods in metabolomics. Here, we focus on results obtained with the UF approach. Multi-scan UF COSY spectra were recorded with signal averaging on a *ca*. 4x4 ppm spectral width (interleaved acquisition methods to improve the spectral width were not sufficiently controlled in 2014). OPLS-DA obtained from the bucketing of UF 2D spectra provided the expected group separation, as for the other 2D methods. Analysis of the loading plots showed that UF COSY provided a better identification of expected biomarkers than 1D NMR, but it was not as efficient as the one obtained with NUS HSQC. This result is consistent with the longer experiment time (35 vs 15 min) of NUS HSQC compared to UF COSY, and also with the better separation capabilities of HSQC.

In 2018, as previously described in section 13.3.2.1, Marchand and co-workers, compared different fast 2D NMR techniques for the untargeted lipidomic fingerprinting on pig serum lipidic extracts, involving two sample groups (ractopamine-fed versus control).[89] In this part we will focus on results obtained with UF COSY approach. Since the authors worked at a relatively high field (700 MHz), interleaved acquisitions (combined with signal averaging) were used to record full UF COSY spectra in 26 min. PLS-DA score plots obtained with UF COSY showed comparable group separation to NUS TOCSY, which was also comparable to 1D NMR in that case. In terms of biomarker identification, UF COSY provided intermediate efficiency between 1D NMR and NUS-accelerated ZQF-TOCSY spectra that lasted 1 h and 47 min for 50% NUS. This is consistent with the fact that UF COSY better separates overlapping peaks than 1D NMR, but is less sensitive than NUS TOCSY. This example highlights that in the case of homonuclear spectroscopy, UF 2D NMR provides an intermediate tool between 1D and NUS-

accelerated 2D experiments, both in terms of efficiency and experiment duration, UF being more high-throughput but also less sensitive than NUS.

In 2018, Gouilleux *et al.* used the same UF strategy to authenticate edible oils with a benchtop NMR spectrometer.[73] The aim was to provide a discrimination of the botanical origin of the oils with a high throughput approach. The authors used a multi-scan strategy to overcome the sensitivity issues related to the use of UF NMR at a medium magnetic field (43 MHz). Interleaving was not required since limited spectral width needed to be sampled at this field. Edible oils of different botanical origins were investigated with multi-scan UF COSY experiments recorded with 72 scans in 2.4 min (see Figure 13.7 (a)). The resulting data were submitted to unsupervised PCA and compared to those obtained from 1D spectra recorded at the same time. A much better group separation was obtained with UF 2D NMR than with 1D NMR as shown in Figures 13.7 (b) and 13.7 (c). This performance was attributed to the ubiquitous peak overlap that characterized benchtop 1D NMR spectra of edible oils at low field. The authors also showed that UF COSY spectra could be used to build a supervised PLS model capable of efficiently detecting the adulteration of olive oil with hazelnut oil. Of course, the use of UF 2D NMR on a benchtop spectrometer would not be suitable for diluted samples, but it can provide an efficient tool for the NMR profiling of complex concentrated samples, such as those encountered in food analysis.

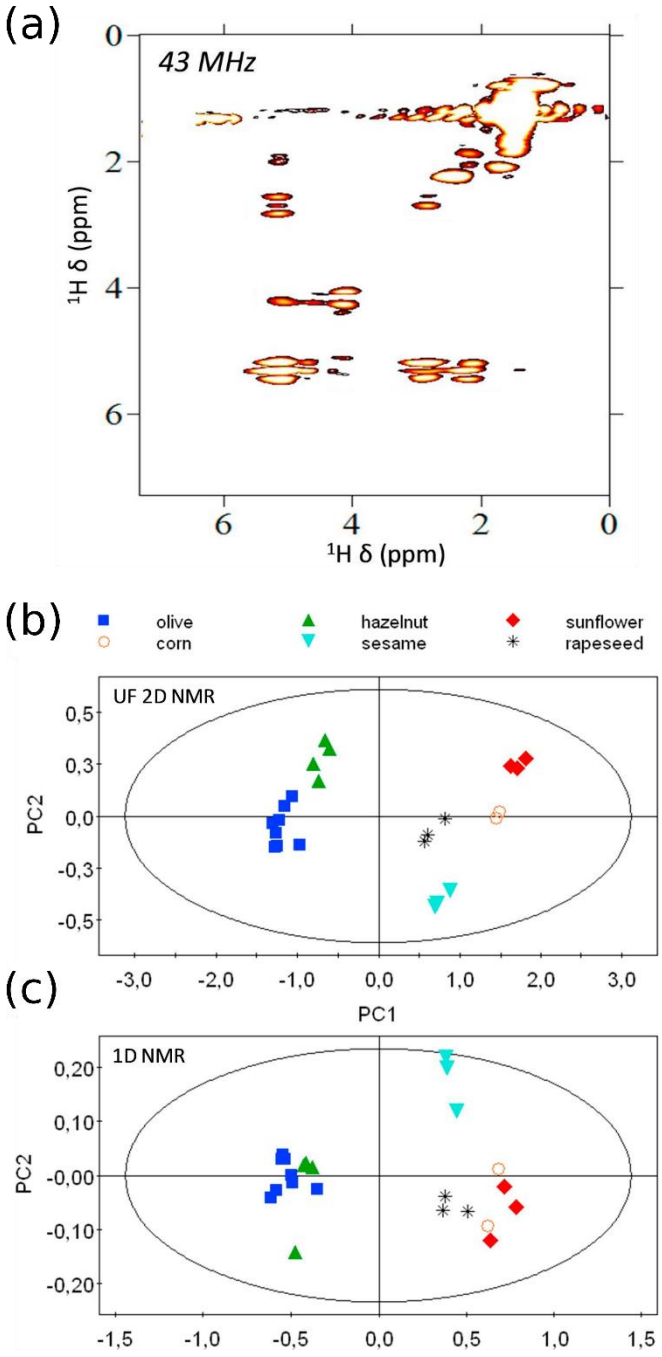

Figure 13.7 Illustration of the potential of 2D experiments for the profiling of food samples with benchtop NMR spectroscopy. (a) Ultrafast 2D COSY spectrum recorded in 2.4 min on a sunflower oil sample in non-deuterated chloroform. PCA analysis on 23 edible oil samples from different botanical origins. (b) PCA score plot from data obtained with the UF 2D NMR experiments and (c) PCA score plot obtained with standard 1D experiments and a variable bucketing approach (5 wide integration regions). Adapted from Ref. [73] with permission from Elsevier, Copyright 2017.

13.3.3.2. Targeted metabolomics

Multi-scan UF COSY experiments were also evaluated for targeted metabolomics by Le Guennec and co-workers.[114] The study aimed at performing a fast determination of absolute metabolite concentrations of 14 major metabolites in model mixtures and then in three breast cancer line extracts from cell cultures. For the model mixture, multiscan UF COSY

experiments were acquired in 10 minutes by averaging 128 scans to obtain convenient sensitivity and to reach the desired limit of quantification for the metabolites studied (at 500 MHz with a cryoprobe). Then, for breast cancer line extract, multiscan UF COSY experiments were recorded in 20 min (256 scans) to detect the lower concentration metabolites. A standard addition procedure was used for quantification, consisting in spiking each sample with a mixture of the 14 targeted analytes. Interestingly, the UF method was able to reach much better repeatability (1 to 4 %) compared to conventional 2D COSY (5.5% to 18.3%). This difference was attributed to spectrometer instabilities that induced t_1 noise in the indirect dimension of conventional experiments, while UF spectra were devoid of such t_1 noise as demonstrated by Pathan *et al*. in 2011 [113]. Concentrations determined for metabolites in cell extracts ranged from 10 to 20 mM for lactate to 0.3 mM for less abundant metabolites. This study highlighted that for concentrations as low as a few hundreds of µM, UF COSY can provide an efficient tool for targeted metabolomics owing to its high repeatability.

Still with the same UF strategy and on targeted metabolomics, Jezequel *et al.* developed a workflow associating multi-scan UF COSY with an external calibration procedure.[74] The goal was to determine the absolute concentration of major metabolites in tomato pericarp extracts. This time, a less time-consuming external calibration method was chosen over standard additions for quantification. A single series of calibration samples containing all the targeted metabolites was designed containing 8 metabolites, with concentrations ranging from 0.1 mmol/L to 150 mmol/L. For the sake of comparison, experiments were performed on 500 and 700 MHz spectrometers equipped with cryoprobes. On the one hand, at 500 MHz, no interleaving scans were needed but more scans needed to be accumulated to provide sufficient SNR (64 scans). On the other hand, 4 interleaved scans were needed at 700 MHz, because the spectral width was even shorter at this field, but less scans were necessary overall to achieve a good sensitivity (16 scans). Therefore, all spectra were recorded in 5 min (see Figure 13.8). The concentration of eight major metabolites was determined with a trueness better than 10 % and a technical repeatability of a few percent. The experiments performed at two magnetic fields led to similar quantitative results, in coherence with the metabolism of tomato fruit. However, two metabolites were not quantified at 500 MHz as their signals were below the limit of quantification. Authors were able to propose biological insights based on the variation of metabolite concentrations at different fruit development stages, suggesting that fast 2D NMR methods formed a promising tool for fast targeted metabolomics of plant samples.

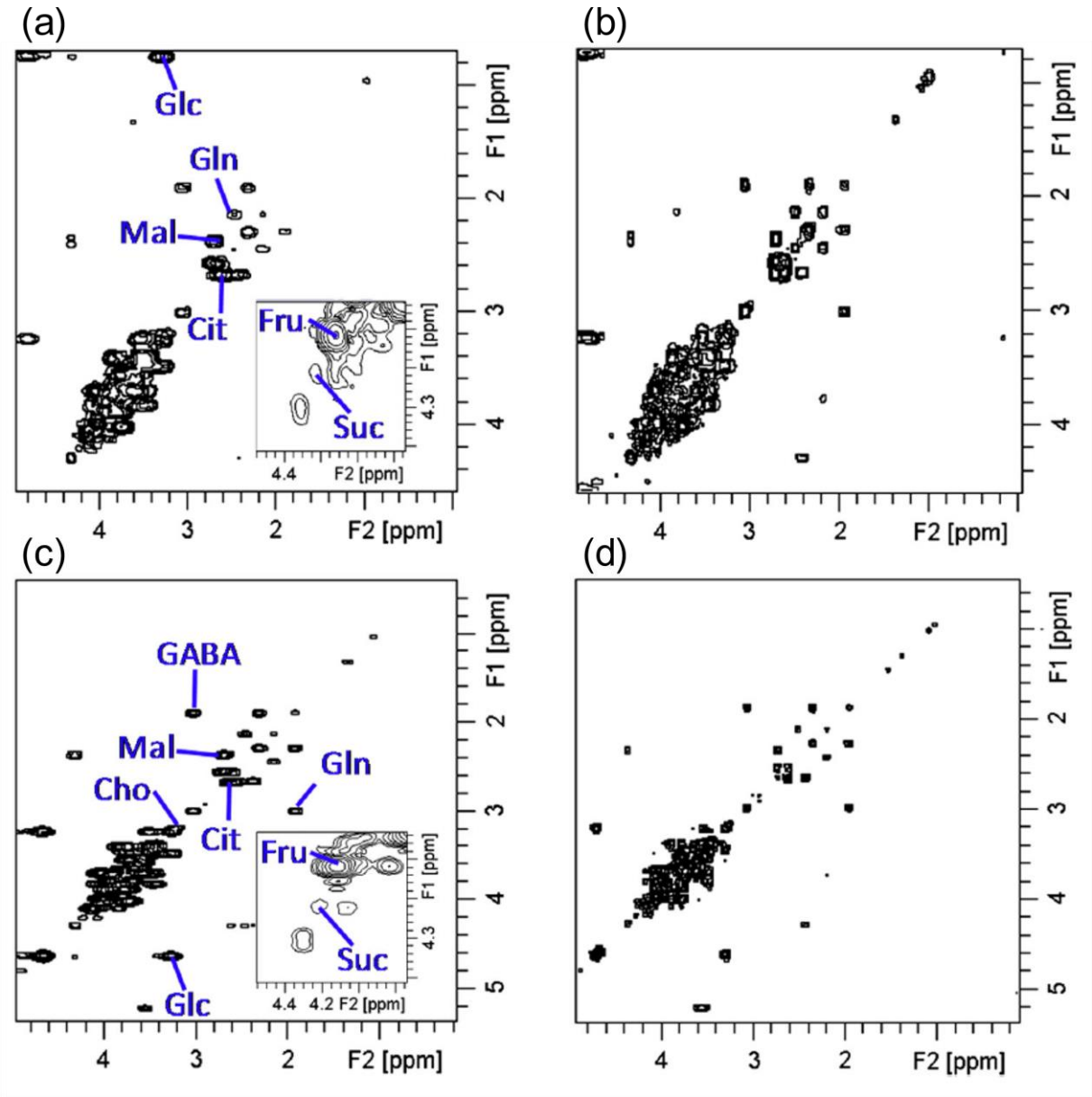

Figure 13.8 Fast multi-scan UF COSY spectra of a tomato fruit pericarp extract recorded in 5 min at 298 K on 500 (a, b) and 700 (c, d) MHz Bruker NMR spectrometers equipped with cryogenically cooled probes. Spectra (b) and (d) were obtained after symmetrizing spectra (a) and (c), respectively. For each major metabolite (glucose, fructose, sucrose, malate, citrate, GABA, glutamine, choline), the peak chosen for quantitative analysis is indicated. Reproduced from Ref. [74] with permission from Springer, Copyright 2015.

13.3.3.3. Fluxomics

Since fluxomics requires high-throughput measurements with a high accuracy, UF NMR could be of interest to the field. In this context, in 2011, Giraudeau and co-workers, evaluated the relevance of UF 2D NMR to measure specific ^{13}C-enrichments in complex mixtures of ^{13}C-labeled metabolites.[115] Model mixtures of ^{13}C-labeled alanine and glucose samples were first used to evaluate the analytical performance of the method, and then a bacterial extract from *E. Coli* was investigated to highlight the potential of the approach in a real case. UF COSY and UF zTOCSY were compared to conventional zTOCSY which was used as a reference method. UF COSY and UF zTOCSY spectra were collected in only 3 minutes each versus 2.5 hours for the conventional zTOCSY. Both UF methods showed an accuracy between 1 to 2 % on the determination of position-specific ^{13}C enrichments, with an average precision of 3% and an excellent linearity. As expected, the sensitivity was lower compared to conventional

zTOCSY spectra recorded in a much longer time, but the relatively high metabolite concentrations were sufficient to measure isotopic enrichments for *ca* 80% of the NMR-detected metabolites. Although potentially providing access to more peaks of interest, UF zTOCSY was found less sensitive than UF COSY due to diffusion effects that occurred during the mixing period, making the spatially encoded procedure less efficient.

To improve the signal discrimination further, this approach was further extended to a 3D experiment called UFJCOSY combining conventional COSY and UF ^{1}H-^{13}C *J*-RES.[116] This approach was tested on isotopically enriched complex samples, a model mixture of alanine and a biomass sample of *E. Coli*. Thanks to the spatial encoding of one dimension, the overall acquisition time to obtain the full 3D map was 11 min, instead of 12 hours if the experiment would have been collected conventionally. This approach was less affected by peak overlapping thanks to the third dimension. Although the analytical performance was not evaluated in this paper, this method could pave the way toward the development of further accelerated 3D methods for the analysis of complex metabolite mixtures.

13.3.3.4 Discussion

As discussed in this section, UF 2D NMR offers an impressive time saving for metabolomics, particularly when considering the need for high throughput methods to deal with sample cohorts in limited time. Since the experiment duration mainly depends on the number of scans (and slightly on the number of interleaved acquisitions), the experiment duration can be tuned to the desired limit of quantification, provided that the overall experiment duration does not exceed 20-30 min. Indeed, longer experiment durations can affect the gradient coil. This limitation, together with the sensitivity limitation of UF 2D NMR, makes it best suited for homonuclear 2D NMR metabolomics, with typical limits of detection in the 0.1 mM – 1 mM range at high field.[61] Heteronuclear UF 2D experiments are not suitable for metabolomics at natural abundance, unless they are combined with hyperpolarization methods as described in section 13.4.2.

13.4 Challenges, limitations and perspectives

13.4.1. Comparison and summary of fast 2D methods

The previous sections illustrate the great variety of metabolomics and fluxomics applications that fast 2D NMR methods have found in the last decade. These examples show both the diversity of fast 2D approaches -and their combination- and the number of biological questions they can address. This literature survey also highlights that each approach has its advantages and drawbacks for metabolomics and fluxomics, as summarized in Table 13.1. The choice of the optimum method for a given research question is not simple, but general tendencies emerge when carefully looking at the literature. Alternative sampling methods such as NUS and aliasing seem the most appropriate methods for heteronuclear 2D NMR metabolomics, while UF 2D NMR is best suited for homonuclear experiments. Therefore, the choice of the optimum approach will depend on the complexity of both the samples being analysed and the biological question being tackled. Tutorial papers have been recently published to help users choosing and optimizing the most appropriate method for both untargeted and targeted metabolomics.[117,118] Hopefully, these will facilitate the use of fast 2D NMR methods in omics workflows by non-expert users.

Table 13.1 Main features of fast 2D NMR methods and their pro and cons for metabolomics and fluxomics

		Pros	Cons
Pulse and delays manipulation strategies	**For all methods**	Reduced recovery delay without compromise on spectral quality.	
	SOFAST	Efficient time saving when dipolar cross-relaxation is efficient.	Selective approach, not generally applicable to mixtures of small molecules. Limited to heteronuclear spectroscopy.
	ALSOFAST and ASAP	Encouraging compatibility with NUS and no need for selective pulses contrary to SOFAST.	Limited to heteronuclear correlation spectroscopy and strong demand on the RF coils due to very short repetition time.
	VRT	Compatible with other time-saving approaches.	Tailored optimization needed.
Sampling strategies or sampling optimization	**Reduced number of t_1 increments**	General approaches applicable to most pulse sequences, easy to setup. Can also be used to record highly resolved spectra.	
	Aliasing	Once conventional 2D is known, easy to setup. Compatible with other time-saving strategies.	Need a priori knowledge of the peak positions. Less adapted to homonuclear 2D NMR (overlap).
	NUS	Easy to setup in commercial software. Compatible with other time-saving strategies.	Sampling scheme and parameters and processing algorithm may require optimization. Less adapted to homonuclear 2D NMR. Repeatability can be disappointing for signals with low SNR.
	Hadamard	Relevant for targeted analysis.	Need a priori knowledge of peak position. Not very easy to set up in practice, optimization needed. Not easily compatible with other time-saving approaches.
Spatial parallelisation	**Ultrafast**	Excellent repeatability of UF homonuclear pulse sequences. Very high-throughput.	Modest sensitivity, limited to homonuclear experiments. Not easy to set up and associated hardware limitations.

13.4.3. Combination of fast 2D NMR and hyperpolarization

As described above, the sensitivity of fast 2D NMR methods in metabolomics remains limited to typical metabolite concentrations above 100 µM for ^{1}H-^{1}H homonuclear experiments. Practical applications require relatively high sample amounts and detection by 2D NMR is often limited to most concentrated metabolites. Combination of hyperpolarization technique with fast 2D approach could be potentially the most efficient solution to circumvent such challenges. Hyperpolarization is an ensemble of techniques that can considerably improve (by several orders of magnitude) the sensitivity of NMR signals. In hyperpolarization methods, non-equilibrium spin population distributions are generated to increase the nuclear spin polarization far beyond thermal equilibrium values, which results in tremendous sensitivity gains.

13.4.3.1. Brief description of hyperpolarization techniques

Among all the hyperpolarization techniques, dynamic nuclear polarization (DNP)[119–122], parahydrogen induced hyperpolarization technique (PHIP)[123–125], and its reversible version, named signal amplification by reversible exchange (SABRE)[126] have shown potential for coupling with fast 2D pulse sequences.

DNP relies on transferring the polarization from the electron spins of a paramagnetic species to the nuclear spins of the sample of interest, a process most efficient when the sample is frozen as a glass in the solid state, at cryogenic temperatures. In order to observe a liquid-state hyperpolarized signal, a dissolution DNP (d-DNP) experiment was suggested in 2003 by Ardenkjaer-Larsen and co-workers[127], where nuclear spins are polarized in the solid state at cryogenic temperatures (typically 1-2 K), in a high magnetic field (3-7 T), followed by rapid dissolution, transfer of the sample to a liquid-state NMR spectrometer and signal acquisition at room temperature.[128,129] Recently, several d-DNP hyperpolarized NMR metabolomics studies showed a huge potential for a wide range of “omics” applications such as targeted and untargeted metabolomics and fluxomics studies.[130–134] The repeatability and robustness of this method enable such applications in biological samples even at sub-millimolar concentrations.

PHIP is generated through the catalytic homogeneous hydrogenation reaction of an unsaturated molecule with hydrogen gas enriched in its para form (p-H_2) resulting in a significant increase in sensitivity. After hydrogenation of an unsaturated and asymmetric molecule, the singlet order of p-H_2 turns into observable magnetization. In contrast to PHIP, the SABRE approach uses a catalyst such that p-H_2 reversibly adds to the catalyst, and the substrate reversibly binds to the catalyst as a ligand. As a result, it offers a rapid and reversible hyperpolarization due to the reversibility of exchange reaction. Introduction of PHIP in NMR metabolomic study has been shown to extend the concentration limit in the nanomolar region for the identification of metabolites present in biological samples.[135]

It is important to highlight that the limited lifetime of hyperpolarization imposes challenges for coupling with conventional 2D NMR which requires a sufficiently long experimental time to sample the indirect dimension with a sufficient resolution. Such challenges are more critical in the case of d-DNP which involves an irreversible process, while SABRE permits renewal of hyperpolarization in between the scans. Indeed, Tessari *et al.* reported SABRE hyperpolarized conventionally acquired homonuclear 2D correlation spectra to analyze biofluid extracts at sub-µM concentration.[136] This is probably the first study which showcases the potential of quantitative analysis using hyperpolarized 2D correlation spectroscopy.

13.4.3.2. Relevant studies combining fast 2D and hyperpolarization techniques

The combination of fast 2D approaches with hyperpolarization in full metabolomic studies is yet to be reported. However, a number of NMR and analytical developments have recently

shown the efficient coupling of fast 2D NMR with hyperpolarization to analyze complex samples, thus paving the way toward further applications in metabolomics. For instance, PHIP-boosted fast 2D techniques such as UF TOCSY spectra of a low concentrated biologically active peptide were acquired within 10 s of experimental time and the sensitivity improved by hyperpolarization reduced the limit of detection by a factor of two. Ultrafast 2D NMR was efficiently coupled with SABRE to obtain 2D COSY spectra of a mixture of analytes at sub-millimolar concentrations.[137] d-DNP combined with fast 2D approaches have also been involved in several analytical applications. Fast 2D experimental strategies have been suggested to sequentially acquire transients with incremented t_1 evolution and phase to obtain d-DNP enhanced 2D spectra from a single hyperpolarized sample.[138] A similar strategy using a small flip angle readout pulse was implemented to record ^{13}C-^{1}H heteronuclear correlations (long-range HSQC and HMQC) in order to detect a range of common metabolites in blood serum. This study reported d-DNP enhanced fast ^{13}C-^{1}H 2D long-range HSQC spectra of ^{13}CO acetylated blood serum with a total signal acquisition time of 9 s.[139] d-DNP boosted Hadamard reconstructed SOFAST-HMQC was also implemented to monitor protein-ligand interactions.[140]

UF methods have also been coupled to d-DNP to explore the potential of UF ^{1}H-^{13}C heteronuclear 2D pulse sequences for analyzing samples at sub-millimolar concentrations.[141] Indeed, although d-DNP provides a huge sensitivity boost to the liquid state NMR signal, such polarization decays exponentially (about 90% ^{1}H hyperpolarization loss in a few seconds) in an irreversible manner. UF 2D NMR is then well suited to exploit such huge polarization gain from d-DNP hyperpolarization before it decays, which, in turn, could solve the general sensitivity issue of UF 2D NMR and even enable the acquisition of ^{1}H-^{13}C 2D correlation spectra at ^{13}C natural abundance in metabolomics. However, rapid sample injection from the polarizer induces turbulent motion of the sample during signal acquisition, which imposes serious practical challenges to gradient-based spatial encoding strategies in UF experiments. Frydman *et. al.* reported optimizations to overcome such issues (such as the choice of dissolution solvent, settling delay before acquisition etc.) and highlighted the possibility to acquire d-DNP enhanced UF 2D ^{15}N-^{1}H and ^{13}C-^{1}H heteronuclear correlation spectra.[142] Further developments reported the sequential acquisition of two UF heteronuclear spectra in a single scan following d-DNP: a short-range ^{1}H-^{13}C spectrum and a long-range ^{1}H-^{13}C correlation spectrum.[143] The same study introduced an elegant solution to incorporate the out-of-the-range ^{13}C resonances into an arbitrary position within the limited spectral range of UF spectra by imparting a tailor-made spatial/spectral encoding scheme. Besides UF heteronuclear 2D pulse sequences, several d-DNP boosted UF ^{1}H-^{1}H homonuclear pulse sequences such as UF COSY, UF TOCSY, and single-quantum/multiple-quantum (SQ-MQ) experiments were reported to analyze complex hyperpolarized mixtures.[144,145] Such developments were made possible thanks to a short transfer time (*ca*. 3 s) between the dissolution of hyperpolarized sample to the collection of the sample in the NMR tube, relying on customized dissolution systems. While metabolomics applications have not been reported yet, recently, a proof-of-concept study identified metabolites from partially enriched and natural abundance extracts of breast cancer cells using d-DNP enhanced UF ^{1}H-^{13}C heteronuclear correlation spectra.[146] As reflected in Figure 13.9 (a) and Figure 13.9 (b) a similar isotopic pattern was reported between a conventional ^{1}H-^{13}C HMBC (heteronuclear multiple bond correlation) spectrum (figure 1a) at thermal equilibrium (*ca.* 14 h of experiment time) and its hyperpolarized counterpart (Figure 13.9 (b)) (*ca.* 30 min of experiment time) recorded on two identical extracts. Figure 13.9 (c) showcases the potential of d-DNP enhanced HMBC experiment at natural abundance in a single scan. However, signals were missing on hyperpolarized UF spectra due to the long transfer time employed in this study. Future improvements relying on fast transfer approaches, combined with this UF 2D NMR strategy, could significantly enhance the potential of this approach for metabolomics.

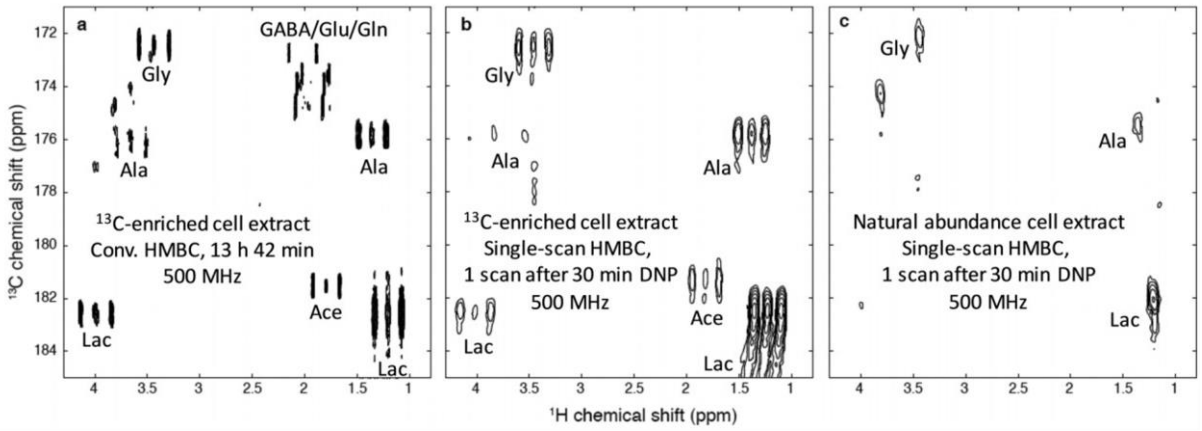

Figure 13.9 $^{1}H \rightarrow ^{13}C$ HMBC-type spectra of extracts of SKBR3 human breast cancer cell lines. (a) Conventional HMBC spectrum, recorded in 13 h 42 min at 500 MHz with a cryogenic probe, on a partially enriched extract (*ca.* 57 million extracted cells) dissolved in 700 µL D_2O. (b) Hyperpolarized single scan spectrum. The cell extract was dissolved in 200 µL of a mixture of H_2O/D_2O/glycerol-d8 (2:3:5) with 25 mM TEMPOL and polarized for 30 min at 1.2 K and 6.7 T, and finally dissolved with 5 mL D_2O. A fraction of 700 µL of the hyperpolarized sample was injected into a 500 MHz spectrometer equipped with a cryogenic probe where the spectrum was recorded in a single scan. (c) Same as (b), but with a natural abundance extract (*ca.* 113 million cells) obtained from the same SKBR3 cell line. Ace: acetate; Ala: alanine; GABA: γ-aminobutyrate; Gln: glutamine; Glu: glutamate; Gly: glycine; Lac: lactate. Reproduced from Ref. [146] with permission from The Royal Society of Chemistry, Copyright 2015.

Overall, the future of hyperpolarization coupled with fast 2D NMR techniques is extremely promising as it shows the potential to circumvent the sensitivity and resolution issues of fast 2D NMR techniques. The above-mentioned examples recorded on complex mixtures support such a perspective. Moreover, several recent developments in hyperpolarized 1D NMR metabolomics (targeted and untargeted) and fluxomics demonstrated that hyperpolarization has the necessary robustness and repeatability for metabolomics studies.[130,131] From these studies, one can anticipate that hyperpolarized fast 2D approaches could considerably strengthen the analysis of hyperpolarized biological samples.

ACKNOWLEDGEMENTS

This work has received funding from the European Research Council (ERC) under the European Union's Horizon 2020 research and innovation program (grant agreements no 801774/DINAMIX and 814747/SUMMIT) and the Region Pays de la Loire (Connect Talent / HPNMR). The authors also acknowledge the French National Infrastructure for Metabolomics and Fluxomics MetaboHUB-ANR-11-INBS-0010 (www.metabohub.fr) and the Corsaire metabolomics core facility (Biogenouest).

References

1. J. K. Nicholson and J. C. Lindon, *Nature*, 2008, **455**, 1054.
2. F. J. Bruggeman and H. V. Westerhoff, *Trends Microbiol.*, 2007, **15**, 45.
3. O. Fiehn, *Plant Mol. Biol.*, 2002, **48**, 155.
4. C. H. Johnson, J. Ivanisevic and G. Siuzdak, *Nat. Rev. Mol. Cell Biol.*, 2016, **17**, 451.
5. U. Sauer, *Mol. Syst. Biol.*, 2006, **52**, 1.
6. M. A. Kamleh, K. Spagou and E. J. Want, *Curr. Pharm. Biotechnol.*, **12**, 976.
7. N. Koen, I. Du Preez and D. T. Loots, in *Advances in Protein Chemistry and Structural Biology*, ed. R. Donev, Academic Press, Cambridge, 1rst edn, 2016.
8. B. Li, X. He, W. Jia and H. Li, *Molecules*, 2017, **22**, 1173.
9. M. Jacob, A. L. Lopata, M. Dasouki and A. M. Abdel Rahman, *Mass Spec. Rev.*, 2019, **38**, 221.
10. M. P. M. Letertre, P. Giraudeau and P. de Tullio, *Frontiers in Molecular Biosciences,* 2021, **8**, 698337.
11. D. S. Wishart, *Nat. Rev. Drug Discov.*, 2016, **15**, 473.
12. D. K. Trivedi, K. A. Hollywood and R. Goodacre, *New Horiz. Transl. Med.*, 2017, **3**, 294.
13. A. Moayyeri, C. J. Hammond, A. M. Valdes and T. D. Spector, *Int. J. Epidemiol.,* 2013, **42**, 76.
14. Q. Chan, R. L. Loo, T. M. D. Ebbels, L. Van Horn, M. L. Daviglus, J. Stamler, J. K. Nicholson, E. Holmes and P. Elliott, *Hypertens. Res.*, 2017, **40**, 336.
15. B. Yu, K. A. Zanetti, M. Temprosa, D. Albanes, N. Appel, C. B. Barrera, Y. Ben-Shlomo, E. Boerwinkle, J. P. Casas, C. Clish, C. Dale, A. Dehghan, A. Derkach, A. H. Eliassen, P. Elliott, E. Fahy, C. Gieger, M. J. Gunter, S. Harada, T. Harris, D. R. Herr, D. Herrington, J. N. Hirschhorn, E. Hoover, A. W. Hsing, M. Johansson, R. S. Kelly, C. M. Khoo, M. Kivimäki, B. S. Kristal, C. Langenberg, J. Lasky-Su, D. A. Lawlor, L. A. Lotta, M. Mangino, L. Le Marchand, E. Mathé, C. E. Matthews, C. Menni, L. A. Mucci, R. Murphy, M. Oresic, E. Orwoll, J. Ose, A. C. Pereira, M. C. Playdon, L. Poston, J. Price, Q. Qi, K. Rexrode, A. Risch, J. Sampson, W. J. Seow, H. D. Sesso, S. H. Shah, X.-O. Shu, G. C. S. Smith, U. Sovio, V. L. Stevens, R. Stolzenberg-Solomon, T. Takebayashi, T. Tillin, R. Travis, I. Tzoulaki, C. M. Ulrich, R. S. Vasan, M. Verma, Y. Wang, N. J. Wareham, A. Wong, N. Younes, H. Zhao, W. Zheng and S. C. Moore, *Am. J. Epidemiol.*, 2019, **188**, 991.
16. D. B. Kell and R. Goodacre, *Drug Discov. Today*, 2014, **19**, 171.
17. V. Tolstikov, *Metabolites*, 2016, **6**, 20.
18. M. Ufer, P.-E. Juif, M.-L. Boof, C. Muehlan and J. Dingemanse, *Expert Opin. Drug Metab. Toxicol.*, 2017, **13**, 803.
19. R. Powers, *J. Med. Chem.*, 2014, **57**, 5860.
20. M. Cuperlovic-Culf and A. S. Culf, *Expert Opin. Drug Discov.*, 2016, **11**, 759.
21. M. Li, B. Wang, M. Zhang, M. Rantalainen, S. Wang, H. Zhou, Y. Zhang, J. Shen, X. Pang, M. Zhang, H. Wei, Y. Chen, H. Lu, J. Zuo, M. Su, Y. Qiu, W. Jia, C. Xiao, L. M. Smith, S. Yang, E. Holmes, H. Tang, G. Zhao, J. K. Nicholson, L. Li and L. Zhao, *PNAS*, 2008, **105**, 2117.
22. C. Noecker, H.-C. Chiu, C. P. MacNally and E. Borenstein, *mSystems*, 2019, **4**, e00579-19.
23. A. Koulman and D. A. Volmer, *Nutr. Bull*., 2008, **33**, 324.

24. J.-L. Sébédio, in *Advances in Food and Nutrition Research*, ed. F. Toldrá, Academic Press, Cambridge, 1rst edn, 2017.
25. I. Garcia-Perez, J. M. Posma, R. Gibson, E. S. Chambers, T. H. Hansen, H. Vestergaard, T. Hansen, M. Beckmann, O. Pedersen, P. Elliott, J. Stamler, J. K. Nicholson, J. Draper, J. C. Mathers, E. Holmes and G. Frost, Lancet Diabetes Endocrinol., 2017, **5**, 184.
26. A. Tebani and S. Bekri, *Front. Nutr.*, 2019, **6**, 41.
27. R. A. Dixon, D. R. Gang, A. J. Charlton, O. Fiehn, H. A. Kuiper, T. L. Reynolds, R. S. Tjeerdema, E. H. Jeffery, J. B. German, W. P. Ridley and J. N. Seiber, *J. Agric. Food Chem.*, 2006, **54**, 8984.
28. R. M. do Prado, C. Porto, E. Nunes, C. L. de Aguiar and E. J. Pilau, *mSystems*, 2018, **3**, e00156-17.
29. C. Motti, *J. Marine Sci. Res. Dev.*, 2012, **2**, e110.
30. E. M. Sogin, E. Puskás, N. Dubilier and M. Liebeke, *mSystems*, 2019, **4**, e00638-19.
31. M. R. Viant, *Metabolomics*, 2009, **5**, 1.
32. C. Bedia, P. Cardoso, N. Dalmau, E. Garreta-Lara, C. Gómez-Canela, E. Gorrochategui, M. Navarro-Reig, E. Ortiz-Villanueva, F. Puig-Castellví and R. Tauler, in Comprehensive Analytical Chemistry, eds. J. Jaumot, C. Bedia and R. Tauler, in *Data Analysis for Omic Sciences: Methods and Applications*, ed. J. Jaumot, C. Bedia and R. Tauler, Elsevier, Amsterdam, 1rst edn, 2018.
33. R. Kumar, A. Bohra, A. K. Pandey, M. K. Pandey and A. Kumar, *Front. Plant Sci.*, 2017, **8**, 1302.
34. C. S. Bloszies and O. Fiehn, *Curr. Opin. Toxicol.*, 2018, **8**, 87.
35. D. I. Walker, D. Valvi, N. Rothman, Q. Lan, G. W. Miller and D. P. Jones, *Curr. Epidemiol. Rep.*, 2019, **6**, 93.
36. L. M. Labine and M. J. Simpson, *Curr. Opin. Environ. Sci. Health*, 2020, **15**, 7.
37. S. Li, Y. Tian, P. Jiang, Y. Lin, X. Liu and H. Yang, *Crit. Rev. Food Sci. Nutr.*, 2021, **61**, 1448.
38. C. Lima, H. Muhamadali and R. Goodacre, *Annu. Rev. Anal. Chem.*, 2021, **14**, 323.
39. J. Martens, G. Berden, R. E. van Outersterp, L. A. J. Kluijtmans, U. F. Engelke, C. D. M. van Karnebeek, R. A. Wevers and J. Oomens, *Sci. Rep.*, 2017, **7**, 3363.
40. M. P. M. Letertre, G. Dervilly and P. Giraudeau, *Anal. Chem.*, 2021, **93**, 500.
41. J. L. Ward, J. M. Baker, S. J. Miller, C. Deborde, M. Maucourt, B. Biais, D. Rolin, A. Moing, S. Moco, J. Vervoort, A. Lommen, H. Schäfer, E. Humpfer and M. H. Beale, *Metabolomics*, 2010, **6**, 263.
42. E. Zelena, W. B. Dunn, D. Broadhurst, S. Francis-McIntyre, K. M. Carroll, P. Begley, S. O'Hagan, J. D. Knowles, A. Halsall, I. D. Wilson and D. B. Kell, *Anal. Chem.*, 2009, **81**, 1357.
43. W. B. Dunn, D. Broadhurst, P. Begley, E. Zelena, S. Francis-McIntyre, N. Anderson, M. Brown, J. D. Knowles, A. Halsall, J. N. Haselden, A. W. Nicholls, I. D. Wilson, D. B. Kell and R. Goodacre, *Nat. Protoc.*, 2011, **6**, 1060.
44. W. B. Dunn, W. Lin, D. Broadhurst, P. Begley, M. Brown, E. Zelena, A. A. Vaughan, A. Halsall, N. Harding, J. D. Knowles, S. Francis-McIntyre, A. Tseng, D. I. Ellis, S. O'Hagan, G. Aarons, B. Benjamin, S. Chew-Graham, C. Moseley, P. Potter, C. L. Winder, C. Potts, P. Thornton, C. McWhirter, M. Zubair, M. Pan, A. Burns, J. K. Cruickshank, G. C. Jayson, N. Purandare, F. C. W. Wu, J. D. Finn, J. N. Haselden, A. W. Nicholls, I. D. Wilson, R. Goodacre and D. B. Kell, *Metabolomics*, 2015, **11**, 9.
45. U. Holzgrabe, R. Deubner, C. Schollmayer and B. Waibel, *J. Pharm. Biomed. Anal.*, 2005, **38**, 806.
46. P. Giraudeau, V. Silvestre and S. Akoka, *Metabolomics*, 2015, **11**, 1041.
47. A. A. Crook and R. Powers, *Molecules*, 2020, **25**, 5128.
48. A.-H. Emwas, R. Roy, R. T. McKay, L. Tenori, E. Saccenti, G. A. N. Gowda, D. Raftery, F. Alahmari, L. Jaremko, M. Jaremko and D. S. Wishart, *Metabolites*, 2019, **9**, 123.
49 J. Hao, M. Liebeke, W. Astle, M. De Iorio, J. G. Bundy and T. M. D. Ebbels, *Nat. Protoc.*, 2014, **9**, 1416.

50. S. Ravanbakhsh, P. Liu, T. C. Bjordahl, R. Mandal, J. R. Grant, M. Wilson, R. Eisner, I. Sinelnikov, X. Hu, C. Luchinat, R. Greiner and D. S. Wishart, *PLoS ONE*, 2015, **10**, e0132873.
51. P. Lacy, R. T. McKay, M. Finkel, A. Karnovsky, S. Woehler, M. J. Lewis, D. Chang and K. A. Stringer, *PLoS ONE*, 2014, **9**, e102929.
52. C. S. Clendinen, B. Lee-McMullen, C. M. Williams, G. S. Stupp, K. Vandenborne, D. A. Hahn, G. A. Walter and A. S. Edison, *Anal. Chem.*, 2014, **86**, 9242.
53. K. Zangger, *Prog. Nucl. Magn. Reson. Spectrosc.*, 2015, **86–87**, 1.
54. J. M. Lopez, R. Cabrera and H. Maruenda, *Sci. Rep.*, 2019, **9**, 6900.
55. Y. Bo, J. Feng, J. Xu, Y. Huang, H. Cai, X. Cui, J. Dong, S. Ding and Z. Chen, *Int. Food Res. J.*, 2019, **125**, 108574.
56. J. Marchand, E. Martineau, Y. Guitton, G. Dervilly-Pinel and P. Giraudeau, *Curr. Opin. Biotechnol.*, 2017, **43**, 49.
57. E. A. Mahrous and M. A. Farag, *J. Adv. Res.*, 2015, **6**, 3.
58. K. Bingol, L. Bruschweiler-Li, D.-W. Li and R. Brüschweiler, *Anal. Chem.*, 2014, **86**, 5494.
59. K. Bingol and R. Brüschweiler, *Anal. Chem.*, 2014, **86**, 47.
60. Q. N. Van, H. J. Issaq, Q. Jiang, Q. Li, G. M. Muschik, T. J. Waybright, H. Lou, M. Dean, J. Uitto and T. D. Veenstra, *J. Proteome Res.*, 2008, **7**, 630.
61. A. L. Guennec, P. Giraudeau and S. Caldarelli, *Anal. Chem.*, 2014, **86**, 5946.
62. B. Féraud, B. Govaerts, M. Verleysen and P. de Tullio, *Metabolomics*, 2015, **11**, 1756.
63. S. L. Robinette, R. Ajredini, H. Rasheed, A. Zeinomar, F. C. Schroeder, A. T. Dossey and A. S. Edison, *Anal. Chem.*, 2011, **83**, 1649.
64. C. Pungaliya, J. Srinivasan, B. W. Fox, R. U. Malik, A. H. Ludewig, P. W. Sternberg and F. C. Schroeder, *PNAS*, 2009, **106**, 7708.
65. J. Alonso, C. Arus, W. M. Westler and J. L. Markley, *Magn. Reson. Med.*, 1989, **11**, 316.
66. I. A. Lewis, S. C. Schommer, B. Hodis, K. A. Robb, M. Tonelli, W. M. Westler, M. R. Sussman and J. L. Markley, *Anal. Chem.*, 2007, **79**, 9385.
67. W. Gronwald, M. S. Klein, H. Kaspar, S. R. Fagerer, N. Nurnberger, K. Dettmer, T. Bertsch and P. J. Oefner, *Anal. Chem.*, 2008, **80**, 9288.
68. P. Giraudeau, *Magn. Reson. Chem.*, 2014, **52**, 259.
69. S. Massou, C. Nicolas, F. Letisse and J.-C. Portais, *Phytochemistry*, 2007, **68**, 2330.
70. S. Massou, C. Nicolas, F. Letisse and J.-C. Portais, *Metab. Eng.*, 2007, **9**, 252.
71. E. Martineau, P. Giraudeau, I. Tea and S. Akoka, *J. Pharm. Biomed. Anal.*, 2011, **54**, 252.
72. P. Giraudeau, N. Guignard, E. Hillion, E. Baguet and S. Akoka, *J. Pharm. Biomed. Anal.*, 2007, **43**, 1243.
73. B. Gouilleux, J. Marchand, B. Charrier, G. S. Remaud and P. Giraudeau, *Food Chem.*, 2018, **244**, 153.
74. T. Jézéquel, C. Deborde, M. Maucourt, V. Zhendre, A. Moing and P. Giraudeau, *Metabolomics*, 2015, **11**, 1231.
75. A. Motta, D. Paris and D. Melck, *Anal. Chem.*, 2010, **82**, 2405.
76. S. Ghosh, A. Sengupta and K. Chandra, *Anal. Bioanal. Chem.*, 2017, **409**, 6731.
77. P. Schanda, Ē. Kupče and B. Brutscher, *J. Biomol. NMR*, 2005, **33**, 199.
78. E. Kupče and R. Freeman, *Magn. Reson. Chem.*, 2007, **45**, 2.
79. D. Schulze-Su, J. Becker and B. Luy, *J. Am. Chem. Soc.*, 2014, **136**, 1242.
80. S. Watermann, C. Schmitt, T. Schneider and T. Hackl, *Metabolites*, 2021, **11**, 39.
81. J. Farjon, C. Milande, E. Martineau, S. Akoka and P. Giraudeau, *Anal. Chem.*, 2018, **90**, 1845.
82. C. Mauve, S. Khlifi, F. Gilard, G. Mouille and J. Farjon, *Chem. Commun.*, 2016, **52**, 6142.
83. S. Macura, *J. Am. Chem. Soc.*, 2009, **131**, 9606.
84. P. M. Le, C. Milande, E. Martineau, P. Giraudeau and J. Farjon, *J. Pharm. Biomed. Anal.*, 2019, **165**, 155.
85. M. P. Schätzlein, J. Becker, D. Schulze-Sünninghausen, A. Pineda-Lucena, J. R. Herance and B. Luy, *Anal. Bioanal. Chem.*, 2018, **410**, 2793.
86. L. Mueller, *J. Biomol. NMR*, 2008, **42**, 129.

87. K. Kazimierczuk, J. Stanek, A. Zawadzka-Kazimierczuk and W. Koźmiński, *Prog. Nucl. Magn. Reson. Spectrosc.*, 2010, **57**, 420.
88. A. Le Guennec, J.-N. Dumez, P. Giraudeau and S. Caldarelli, *Magn. Reson. Chem.*, 2015, **53**, 913.
89. J. Marchand, E. Martineau, Y. Guitton, B. Le Bizec, G. Dervilly-Pinel and P. Giraudeau, *Metabolomics*, 2018, **14**, 60.
90. B. Féraud, E. Martineau, J. Leenders, B. Govaerts, P. de Tullio and P. Giraudeau, *Metabolomics*, 2020, **16**, 42.
91. B. Féraud, J. Leenders, E. Martineau, P. Giraudeau, B. Govaerts and P. de Tullio, *Metabolomics*, 2019, **15**, 63.
92. J. C. J. Barna, E. D. Laue, M. R. Mayger, J. Skilling and S. J. P. Worrall, *J. Magn. Reson. (1969)*, 1987, **73**, 69.
93. C. Ludwig, D. G. Ward, A. Martin, M. R. Viant, T. Ismail, P. J. Johnson, M. J. O. Wakelam and U. L. Günther, *Magn. Reson. Chem.*, 2009, **47**, S68.
94. D. Jeannerat, in *Encyclopedia of Magnetic Resonance*, ed. R. K. Harris and R. E. Wasylishen, John Wiley & Sons, Ltd, Chichester, 1rst edn, 2011.
95. E. Martineau, I. Tea, S. Akoka and P. Giraudeau, *NMR Biomed.*, 2012, **25**, 985.
96. T. von Schlippenbach, P. J. Oefner and W. Gronwald, *Sci. Rep.*, 2018, **8**, 4249.
97. L. Jiang, K. Howlett, K. Patterson and B. Wang, *Anal. Biochem.*, 2020, **597**, 113692.
98. B. Zhang, R. Powers and E. M. O'Day, *Metabolites*, 2020, **10**, 203.
99. R. K. Rai and N. Sinha, *Anal. Chem.*, 2012, **84**, 10005.
100. R. K. Rai, P. Tripathi and N. Sinha, *Anal. Chem.*, 2009, **81**, 10232.
101. Y. Sekiyama and J. Kikuchi, *Phytochemistry*, 2007, **68**, 2320.
102. E. Cahoreau, L. Peyriga, J. Hubert, F. Bringaud, S. Massou and J.-C. Portais, *Anal. Biochem.*, 2012, **427**, 158.
103. S. Lee, H. Wen, Y. J. An, J. W. Cha, Y.-J. Ko, S. G. Hyberts and S. Park, *Anal. Chem.*, 2017, **89**, 1078.
104. T. Jézéquel, V. Joubert, P. Giraudeau, G. S. Remaud and S. Akoka, *Magn. Reson. Chem.*, 2017, **55**, 77.
105. N. Merchak, V. Silvestre, L. Rouger, P. Giraudeau, T. Rizk, J. Bejjani and S. Akoka, *Talanta*, 2016, **156–157**, 239.
106. E. Martineau, S. Akoka, R. Boisseau, B. Delanoue and P. Giraudeau, *Anal. Chem.*, 2013, **85**, 4777.
107. L. Haddad, S. Renou, G. S. Remaud, T. Rizk, J. Bejjani and S. Akoka, *Anal. Bioanal. Chem.*, 2021, **413**, 1521.
108. J.-N. Dumez, *Prog. Nucl. Magn. Reson. Spectrosc.*, 2018, **109**, 101.
109. L. Frydman, T. Scherf and A. Lupulescu, *PNAS*, 2002, **99**, 15858.
110. P. Giraudeau and L. Frydman, *Annu. Rev. Anal. Chem.*, 2014, **7**, 129.
111. C. Lhoste, B. Lorandel, C. Praud, A. Marchand, R. Mishra, A. Dey, A. Bernard, J.-N. Dumez and P. Giraudeau, *Prog. Nucl. Magn. Reson. Spectrosc.*, 2022, **130-131**, 1.
112. S. Akoka and P. Giraudeau, *Magn. Reson. Chem.*, 2015, **53**, 986.
113. M. Pathan, S. Akoka, I. Tea, B. Charrier and P. Giraudeau, *Analyst*, 2011, **136**, 3157.
114. A. Le Guennec, I. Tea, I. Antheaume, E. Martineau, B. Charrier, M. Pathan, S. Akoka and P. Giraudeau, *Anal. Chem.*, 2012, **84**, 10831.
115. P. Giraudeau, S. Massou, Y. Robin, E. Cahoreau, J.-C. Portais and S. Akoka, *Anal. Chem.*, 2011, **83**, 3112.
116. P. Giraudeau, E. Cahoreau, S. Massou, M. Pathan, J.-C. Portais and S. Akoka, *ChemPhysChem*, 2012, **13**, 3098.
117. E. Martineau, J.-N. Dumez and P. Giraudeau, *Magn. Reson. Chem.*, 2020, **58**, 390.
118. E. Martineau, in *NMR-Based Metabolomics: Methods and Protocols*, ed G. A. Nagana Gowda and D. Raftery, Springer, New York, 2019, 20, 365.
119. A. W. Overhauser, *Phys. Rev.*, 1953, **92**, 411.
120. T. R. Carver and C. P. Slichter, *Phys. Rev.*, 1953, **92**, 212.
121. A. S. Lilly Thankamony, J. J. Wittmann, M. Kaushik and B. Corzilius *Prog. Nucl. Magn. Reson. Spectrosc.*, 2017, **102–103**, 120.

122. M. Goldman, *Appl. Magn. Reson.*, 2008, **34**, 219.
123. M. G. Pravica and D. P. Weitekamp, *Chem. Phys. Lett.*, 1988, **145**, 255.
124. J. Natterer and J. Bargon, *Prog. Nucl. Magn. Reson. Spectrosc.*, 1997, **31**, 293.
125. C. R. Bowers and D. P. Weitekamp, *Phys. Rev. Lett.*, 1986, **57**, 2645.
126. R. W. Adams, J. A. Aguilar, K. D. Atkinson, M. J. Cowley, P. I. P. Elliott, S. B. Duckett, G. G. R. Green, I. G. Khazal, J. López-Serrano and D. C. Williamson, *Science*, 2009, **323**, 1708.
127. J. H. Ardenkjær-Larsen, B. Fridlund, A. Gram, G. Hansson, L. Hansson, M. H. Lerche, R. Servin, M. Thaning and K. Golman, *PNAS*, 2003, **100**, 10158.
128. J. H. Ardenkjaer-Larsen, *J. Magn. Reson.*, 2016, **264**, 3.
129. S. Jannin, J.-N. Dumez, P. Giraudeau and D. Kurzbach, *J. Magn. Reson.*, 2019, **305**, 41.
130. A. Bornet, M. Maucourt, C. Deborde, D. Jacob, J. Milani, B. Vuichoud, X. Ji, J.-N. Dumez, A. Moing, G. Bodenhausen, S. Jannin and P. Giraudeau, *Anal. Chem.*, 2016, **88**, 6179.
131. A. Dey, B. Charrier, E. Martineau, C. Deborde, E. Gandriau, A. Moing, D. Jacob, D. Eshchenko, M. Schnell, R. Melzi, D. Kurzbach, M. Ceillier, Q. Chappuis, S. F. Cousin, J. G. Kempf, S. Jannin, J.-N. Dumez and P. Giraudeau, *Anal. Chem.*, 2020, **92**, 14867.
132. M. H. Lerche, D. Yigit, A. B. Frahm, J. H. Ardenkjær-Larsen, R. M. Malinowski and P. R. Jensen, *Anal. Chem.*, 2018, **90**, 674.
133. A. B. Frahm, P. R. Jensen, J. H. Ardenkjær-Larsen, D. Yigit and M. H. Lerche, *J. Magn. Reson.*, 2020, **316**, 106750.
134. A. B. Frahm, D. Hill, S. Katsikis, T. Andreassen, J. H. Ardenkjær-Larsen, T. F. Bathen, S. A. Moestue, P. R. Jensen and M. H. Lerche, *Talanta*, 2021, **235**, 122812.
135. L. Sellies, I. Reile, R. L. E. G. Aspers, M. C. Feiters, F. P. J. T. Rutjes and M. Tessari, *Chem. Commun.*, 2019, **55**, 7235.
136. I. Reile, N. Eshuis, N. K. J. Hermkens, B. J. A. van Weerdenburg, M. C. Feiters, F. P. J. T. Rutjes and M. Tessari, *Analyst*, 2016, **141**, 4001.
137. V. Daniele, F.-X. Legrand, P. Berthault, J.-N. Dumez and G. Huber, *ChemPhysChem*, 2015, **16**, 3413.
138. H. Zeng, S. Bowen and C. Hilty, *J. Magn. Reson.*, 2009, **199**, 159.
139. S. Katsikis, I. Marin-Montesinos, C. Ludwig and U. L. Günther, *J. Magn. Reson.*, 2019, **305**, 175.
140. Y. Wang, J. Kim and C. Hilty, *Chem. Sci.*, 2020, **11**, 5935.
141. L. Frydman and D. Blazina, *Nature Phys*, 2007, **3**, 415.
142. M. Mishkovsky and L. Frydman, *ChemPhysChem*, 2008, **9**, 2340.
143. P. Giraudeau, Y. Shrot and L. Frydman, *J. Am. Chem. Soc.*, 2009, **131**, 13902.
144. R. Panek, J. Granwehr, J. Leggett and W. Köckenberger, *Phys. Chem. Chem. Phys.*, 2010, **12**, 5771.
145. K. Singh, C. Jacquemmoz, P. Giraudeau, L. Frydman and J.-N. Dumez, *Chem. Commun.*, 2021, **57**, 8035.
146. J.-N. Dumez, J. Milani, B. Vuichoud, A. Bornet, J. Lalande-Martin, I. Tea, M. Yon, M. Maucourt, C. Deborde, A. Moing, L. Frydman, G. Bodenhausen, S. Jannin and P. Giraudeau, *Analyst*, 2015, **140**, 5860.